Supporting Information

Visualization and Quantification of Drug Release by GSH-Responsive Multimodal Integrated Micelles

Long Xiao[a,b+], Lei Zhang[a,b+], Sha Li[a], Yue Zhu[a], Qiao Yu[a], Zhaoqing Liu[a,b], Maosong Qiu[a,b], Yu Li[a,b], Shizhen Chen[a,b,c*], Xin Zhou[a,b,c*]

[a] State Key Laboratory of Magnetic Resonance and Atomic and Molecular Physics, National Center for Magnetic Resonance in Wuhan, Wuhan Institute of Physics and Mathematics, Innovation Academy for Precision Measurement Science and Technology, Chinese Academy of Sciences, Wuhan 430071, P. R. China.

[b] University of Chinese Academy of Sciences, Beijing 100049, P. R. China.

[c] School of Biomedical Engineering, Hainan University, Haikou, Hainan 570228, China.

* Corresponding author: xinzhou@wipm.ac.cn; chenshizhen@wipm.ac.cn.

[+] These authors contributed equally to this work

Table of Contents

1. Materials and Characterization

4-Aminobenzotrifluoride, stannous chloride dihydrate, concentrated hydrochloric acid, sodium nitrite, 3-methyl-2-butanone, 1,3-propane sultone, and sodium hydride was purchased from J&K Scientific Ltd. 4-Hydroxycyclohexanone , 1,4-cyclohexanediol, 3-bromopropyne, pyridinium chlorochromate, and phosphorus oxychloride were purchased from Sigma-Aldrich. N-(3-dimethylaminopropyl)-n''-ethylcarbodiimide hydrochloride (EDCI), N-hydroxysulfosuccinimide (NHS), cystamine dihydrochloride, azidoacetic acid, 3-(Tritylthio)propanoicacid, N,N-Diisopropylethylamine, gemcitabine, O-(Benzotriazol-1-yl)-N,N,N",N"-tetramethyluronium tetrafluoroborate (TBTU), triethylsilane, trifluoroacetic acid (TFA), 2,2′-Dipyridyldisulfide were purchased from Leyan. Phenyl isothiocyanate (PEITC) was purchased from MACKLIN reagent. 4,6-Diamino-2-phenyl indole, mPEG-COOH (Mw = 2000), mPEG-SH (Mw = 1000), and dialysis bags used here (cut off Mw = 1000/5000/10000) were obtained from Shyuanye Biotechnology Corporation. All the other solvents and reagents were of analytical grade and obtained from Sinopharm Chemical Reagent Co., Ltd. Dimethyl formamide (DMF), ethanol, dichloromethane, and methanol were purified using standard methods. Other reagents and solvents were of commercial quality without further purification. Water used in this study was deionized with a Milli-QSP reagent water system (Millipore) to a specific resistivity of 18.4 MΩ·cm. A549 cells originated from the Institute of Biochemistry and Cell Biology, which were cultured in F12K Medium (Hyclone) with 10% fetal bovine serum (FBS, Sangon, Shanghai, China) at 37°C with 5% CO_2.

The ultraviolet-visible (UV-vis) absorption spectra were recorded using an Evolution 220 UV-vis spectrophotometer (ThermoFisher Scientific). Fluorescence spectra were measured on an FS5 fluorescence spectrometer (EDINBURGH INSTRUMENTS). Dynamic light scattering (DLS) was performed with a Malvern Zetasizer Nano ZS90 machine containing a He−Ne laser. The measurement was carried out at 25°C, and the scattering angle was fixed at 90°. Mass spectra were obtained on a Liquid Chromatography Triple Quadrupole Mass Spectrometry (LC-MS/MS) in Agilent Technologies. The morphology was measured by transmission electron microscopy (TEM) performed on a Hitachi S-4800 with an electron microscope operating at acceleration voltages of 100 kV using 4% phosphotungstate acid (PTA) for micellar positive stain. ^{1}H, ^{13}C, and ^{19}F NMR spectra were recorded on a Bruker AVANCE III TM 500 MHz spectrometer and referenced to the

solvent peak. ^{1}H MRI and ^{19}F MRI were measured on Bruker 400 MHz wide-bore nuclear magnetic resonance spectrometer. *In vivo* fluorescence imaging was performed with small animals living fluorescence imaging system by PerkinElmer Co. Ltd.

2. Synthesis of PEG-SS-FCy7 and PEG-SS-GEM

PEG-SS-FCy7 (PSF) and PEG-SS-GEM (PSG) are independent block copolymers, and the exhaustive synthetic route is shown in Figure S1. NMR and mass spectrometry were used to characterize the chemical structures of the products of each step.

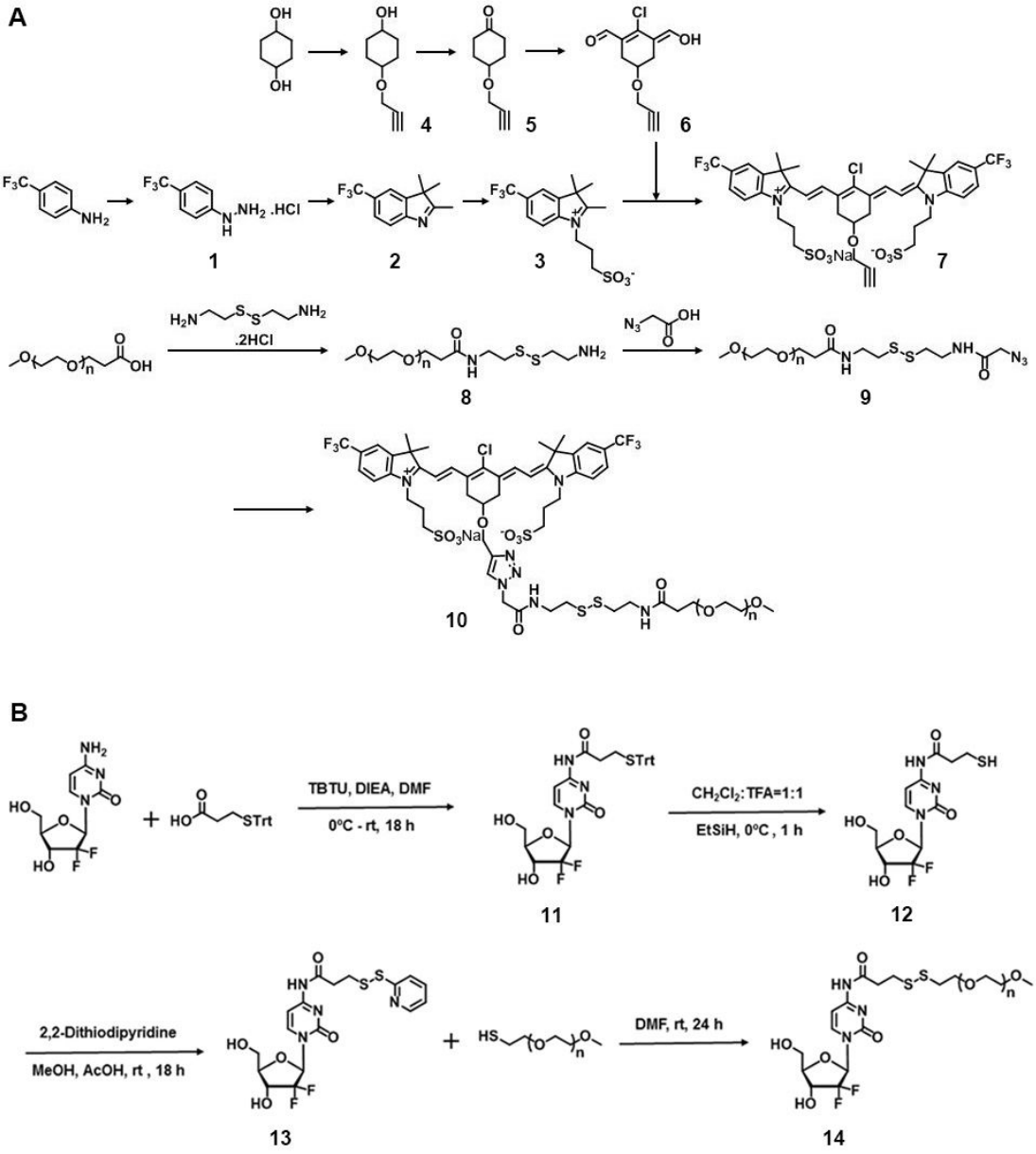

Figure S1. Synthetic routes of (A) redox-responsive bimodal contrast agent PEG-SS-FCy7 (PSF) and (B) polymeric prodrug micelle PEG-SS-GEM (PSG).

Synthesis of Compound 1. 4-Aminobenzotrifluoride (32.2 g, 0.2 mol) was dissolved in 200 mL of concentrated hydrochloric acid (12 mol/L), and the reaction was stirred for 30 min at room temperature. Then the reaction was transferred to a low-temperature reaction bath (-25°C) and stirred for 10 min. $NaNO_2$ (16.5 g, 0.24 mol) was dissolved in pure water (90 mL) and added dropwise with a constant pressure drop funnel. Then the reaction continued to stir for 1 h. Subsequently, stannous chloride dihydrate (112.8 g, 0.5 mol) was dissolved in 150 mL of concentrated hydrochloric acid and added slowly to the reaction mixture. After stirring for 10 min, the reaction was transferred to room temperature and stirred for 1 h. After filtration, the residue was washed with concentrated hydrochloric acid, ether, and dichloromethane. Finally, the solvent was removed by a rotary evaporator and concentrated *in vacuo* to obtain compound **1** as a light pink solid (38.5 g, 90.7% yield).

^{1}H NMR (500 MHz, CD_3OD) δ 7.63 (d, J = 8.5 Hz, 1H), 7.13 (d, J = 8.5 Hz, 1H). ^{13}C NMR (126 MHz, CD_3OD) δ 148.16, 126.31, 125.49, 123.75, 121.20. ^{19}F NMR (471 MHz, CD_3OD) δ -63.25 (s). HRMS (ESI) calc for $C_7H_7N_2F_3$, $[M+H]^+$ = 177.06341, found 177.06462 (Figure S26-S29).

Synthesis of Compound 2. Compound **1** (17.7 g, 0.1 mol) and 3-methyl-2-butanone (26.0 g, 0.3 mol) were stirred at 150 mL of methanol and 3 mL of concentrated hydrochloric acid at 90°C for 10 h under N_2 atmosphere. After cooling to room temperature, the solvent was removed under reduced pressure. And the residue was dissolved with CH_2Cl_2. The organic phase was washed with 1 M $NaHCO_3$ aqueous solution until there were no bubbles, and the organic layer was collected and dried over anhydrous sodium sulfate. After filtration, the solvent was concentrated, and the residue was purified by column chromatography (ethyl acetate: n-hexane = 1: 10, v/v) to afford compound **2** as a reddish oil (18.6 g, 81.9% yield).

^{1}H NMR (500 MHz, CD_3OD) δ 7.63 (s, 2H), 7.54 (s, 1H), 7.28 (s, 1H), 1.36 (s, 4H), 1.28 (s, 3H). ^{13}C NMR (126 MHz, CD_3OD) δ 191.24, 156.28, 146.10, 128.43, 126.97, 123.49, 118.45, 54.07, 29.71, 22.79, 15.63. ^{19}F NMR (471 MHz, CD_3OD) δ -61.34 (s). HRMS (ESI) calc for $C_{12}H_{12}NF_3$, $[M+H]^+$ = 228.09946, found 228.09941 (Figure S30-S33).

Synthesis of Compound 3. Compound **2** (15.0 g, 70 mmol) and 1,3-propane sultone (21.3 g, 180 mmol) were suspended in 1,2-dichlorobenzene (100 mL) and stirred at 110°C overnight under an N_2 atmosphere. After cooling to room temperature, the reaction was filtrated and washed with CH_2Cl_2 three times. The residue was purified by column chromatography (CH_3OH: CH_2Cl_2 = 1: 4, v/v). Compound **3** was obtained as a pink solid (13.8 g, 56.5% yield).

^{1}H NMR (500 MHz, CD_3OD) δ 8.30 – 8.15 (m, 1H), 8.01 (d, *J* = 8.4 Hz, 1H), 4.87 (s, 2H), 4.84 – 4.67 (m, 1H), 3.37 (s, 1H), 3.12 – 2.96 (m, 1H), 2.51 – 2.34 (m, 1H), 1.69 (s, 3H), 1.35 (t, *J* = 27.7 Hz, 1H). ^{13}C NMR (126 MHz, CD_3OD) δ 200.43, 144.01, 143.00, 131.53, 131.40, 126.76, 126.73, 124.81, 122.65, 120.65, 116.30, 55.18, 23.06, 21.10. ^{19}F NMR (471 MHz, CD_3OD) δ -63.53 (s). HRMS (ESI) calc for $C_{15}H_{18}NSO_3F_3$ $[M-H]^-$ = 348.08867, found 348.09168 (Figure S34-S37).

Synthesis of Compound 4. NaH (mass fraction 60%, 30.0 g, 0.75 mol) was added into a 500 mL round-bottomed flask, 200 mL of anhydrous DMF to disperse, and stirred in an ice-water bath. 1,4-cyclohexanediol (58.0 g, 0.5 mol) was dissolved in 100 mL of anhydrous DMF and then slowly added to the above reaction solution with a constant pressure dropping funnel, and the reaction was continued for 3 h after the addition was completed. 3-Bromopropyne (50 mL) was dissolved in 50 mL of anhydrous toluene and then added dropwise to the above reaction solution with a constant pressure dropping funnel and reacted overnight. After the reaction, ultrapure water was added dropwise to the solution to terminate the reaction until no bubbles were generated. The solvent was removed with a rotary evaporator, and 300 mL of CH_2Cl_2 was added to the round-bottomed flask to dissolve. The filtrate was retained, concentrated, and purified by column chromatography (ethyl acetate: n-hexane = 1: 1, v/v) to obtain a white solid (22.4 g, yield 29.1%).

^{1}H NMR (500 MHz, CD_3OD) δ 4.16 (d, *J* = 2.5 Hz, 1H), 3.73 (dd, *J* = 7.8, 3.7 Hz, 1H), 3.69 – 3.57 (m, 1H), 2.40 (dd, *J* = 6.0, 3.5 Hz, 1H), 2.03 (s, 1H), 1.95 – 1.76 (m, 1H), 1.66 (dd, *J* = 7.5, 4.0 Hz, 1H), 1.57 (s, 1H), 1.34 (s, 1H). ^{13}C NMR (126 MHz, CD_3OD) δ 80.38, 77.34, 77.08, 76.83, 73.86, 55.17, 32.46, 28.97, 27.19. HRMS (ESI) calc for $C_9H_{14}O_2$ $[M+H]^+$ = 155.10666, found 155.10686 (Figure S38-S40).

Synthesis of Compound 5. Pyridinium chlorochromate (PCC, 21.5 g, 100 mmol) was added to 150 mL of CH_2Cl_2 and stirred at room temperature. Compound **4** (14.0 g, 90 mmol) was dissolved with 30 mL of CH_2Cl_2 and slowly added dropwise to the above reaction solution with a constant pressure dropping funnel, and reacted at room temperature overnight. After the reaction, the mixture was filtered, and the filtrate was extracted with CH_2Cl_2/H_2O. The organic phase was separated, kept, and washed with pure water thrice. The solvent was removed by a rotary evaporator, and the residue was purified by column chromatography (ethyl acetate: n-hexane = 1: 15, v/v) to obtain a pale yellow oil (12.9 g, 93.7% yield).

^{1}H NMR (500 MHz, CD_3OD) δ 4.23 (d, J = 2.4 Hz, 1H), 3.95 (s, 1H), 2.56 (s, 1H), 2.45 (t, J = 2.4 Hz, 1H), 2.26 (d, J = 14.8 Hz, 1H), 2.09 (dd, J = 13.3, 5.9 Hz, 1H), 2.01 – 1.86 (m, 1H). ^{13}C NMR (126 MHz, CD_3OD) δ 210.84, 79.88, 78.54, 77.36, 75.89, 74.34, 72.05, 55.68, 30.28. HRMS (ESI) calc for $C_9H_{12}O_2$ $[M+Na]^+$ = 175.07295, found 175.07339 (Figure S41-S43).

Synthesis of Compound 6. Anhydrous DMF (15 mL) was added in a 100 mL round bottom flask at 0°C. Then $POCl_3$ (15 mL, 160 mmol) was slowly added and stirred for 30 min. Next, compound **5** (7.4 g, 48 mmol) was added by syringe, and the reaction was stirred at 60°C for 3 h. After cooling to room temperature, the red mixture was poured into 300 g ice and stood overnight. The yellow precipitate was collected, washed with H_2O, and triturated with CH_2Cl_2. The product was collected by filtration and dried *in vacuo* to obtain compound **6** as a luminous yellow powder (7.7 g, 45.8% yield).

^{1}H NMR (500 MHz, DMSO-d6) δ 10.12 (s, 1H), 7.36 (s, 1H), 4.14 (d, J = 2.4 Hz, 2H), 3.91 (s, 4H), 3.41 (d, J = 1.0 Hz, 1H), 2.60 – 2.55 (m, 2H), 2.42 (dd, J = 17.0, 5.8 Hz, 1H). ^{13}C NMR (126 MHz, CD_3OD) δ 190.00, 154.97, 148.91, 145.31, 127.01, 125.60, 111.51, 110.64, 102.94, 79.40, 74.24, 70.71, 54.64, 28.57. HRMS (ESI) calc for $C_8H_9O_2Cl$ $[M+H]^+$ = 227.04695, found 227.04448 (Figure S44-46).

Synthesis of Compound 7 (FCy7). Compound **3** (5.2 g, 15 mmol), compound **6** (1.7 g, 7.5 mmol), and anhydrous sodium acetate (0.6 g, 7.5 mmol) were added in acetic anhydride (60 mL) and stirred at 60°C overnight under N_2 atmosphere. After cooling to room temperature, the mixture was

precipitated with Et_2O and dried *in vacuo*. The crude product was purified by column chromatography (CH_3OH: CH_2Cl_2 = 1: 4, v/v). The product was dried *in vacuo* to obtain compound **7** as dark green with metallic gloss solid (3.4 g, 51.1% yield).

^{1}H NMR (500 MHz, DMSO-d6) δ 8.35 (d, *J* = 13.8 Hz, 1H), 8.08 (s, 1H), 7.77 (dd, *J* = 22.4, 8.2 Hz, 2H), 6.67 (d, *J* = 14.0 Hz, 1H), 4.48 (s, 2H), 4.37 (s, 1H), 4.08 (s, 1H), 3.59 (s, 1H), 3.44 (s, 1H), 3.17 (s, 1H), 3.02 (d, *J* = 13.7 Hz, 1H), 2.91 (s, 1H), 2.64 (t, *J* = 5.8 Hz, 2H), 2.08 (s, 2H), 1.73 (d, *J* = 4.4 Hz, 6H). ^{13}C NMR (126 MHz, DMSO-d6) δ 173.82, 148.96, 145.54, 142.50, 128.14, 126.82, 125.98, 125.42, 123.82, 121.66, 120.28, 112.50, 103.53, 81.46, 77.51, 70.45, 55.85, 49.62, 49.06, 48.09, 43.58, 31.41, 27.74, 23.85. ^{19}F NMR (471 MHz, DMSO-d6) δ -59.68 (s). HRMS (ESI) calc for $C_{41}H_{42}N_2O_7F_6S_2Cl$ $[M]^-$ = 887.20316, found 887.20701 (Figure S47-50).

Synthesis of Compound 8. Methoxy polyethylene glycol carboxyl group (mPEG-COOH, Mw = 2000, 900 mg) was added to a 50 mL round-bottom flask, add 15 mL of anhydrous DMSO to the round-bottom flask, and then N-hydroxysulfosuccinimide (NHS, 324 mg, 2.8 mmol) and 1-(3-dimethylaminopropyl)-3-ethylcarbodiimide hydrochloride (EDCI, 116.5 mg, 0.6 mmol) were added and reacted in the dark for 1 h. Cystamine dihydrochloride (710 mg, 3.1 mmol) and pyridine (0.5 mL) were dissolved in 5 mL of anhydrous DMSO, then added dropwise to the above reaction solution, and reacted at room temperature for 24 h. After the reaction, 20 mL of pure water was added and dialyzed with a dialysis bag with a molecular weight cut-off of Mw = 1000 for 24 hours (water was replaced at the 2, 6, and 12 h, respectively). When the dialysis was completed, the liquid in the dialysis bag was collected and lyophilized to obtain a white solid powder (712.2 mg, 74.1% yield).

^{1}H NMR (500 MHz, CD_3OD) δ 4.27 – 4.20 (m, 1H), 3.82 (s, 1H), 3.70 – 3.61 (m, 88H), 3.38 (s, 1H), 3.03 (t, *J* = 7.0 Hz, 1H), 2.90 (t, *J* = 6.7 Hz, 1H), 2.67 (t, *J* = 6.7 Hz, 1H), 2.60 (d, *J* = 6.6 Hz, 1H), 2.53 (d, *J* = 6.8 Hz, 1H). ^{13}C NMR (126 MHz, CD_3OD) δ 173.09, 172.87, 71.59, 70.09, 68.73, 63.33, 61.49, 60.45, 57.72, 31.71, 27.95. (Figure S51-S52)

Synthesis of Compound 9. Azidoacetic acid (22 mg, 0.22 mmol) was added into a 25 mL round-bottomed flask with 5 mL of anhydrous DMSO, and then NHS (230 mg, 2.0 mmol) and EDCI (58

mg, 0.3 mmol) were added and stirred until the solution was clear. The solution was reacted in a dark environment for 1 h. The white solid powder prepared in step 8 (550 mg) and pyridine (0.5 mL) were dissolved in 5 mL of anhydrous DMSO and added dropwise to the above reaction solution at room temperature. The reaction was carried out for 24 h. When the reaction finished, 20 mL of pure water was added, and the dialysis bag with molecular weight cut-off Mw = 1000 was used for dialysis for 24 h (the water was replaced at 2, 6, and 12 h, respectively). After the dialysis, the liquid in the dialysis bag was collected for freezing dry to obtain a white solid powder (487.1 mg, 84.6% yield).

^{1}H NMR (500 MHz, CD_3OD) δ 4.28 – 4.20 (m, 1H), 3.93 (s, 1H), 3.83 – 3.77 (m, 1H), 3.71 (s, 1H), 3.69 – 3.59 (m, 70H), 3.59 – 3.53 (m, 2H), 3.54 – 3.48 (m, 1H), 3.38 (s, 1H), 2.91 – 2.82 (m, 1H), 2.62 (ddd, *J* = 11.4, 10.0, 4.0 Hz, 2H), 2.53 (t, *J* = 7.0 Hz, 1H), 2.18 (s, 1H), 1.20 (t, *J* = 7.1 Hz, 1H). ^{13}C NMR (126 MHz, CD_3OD) δ 172.83, 71.59, 70.20, 68.69, 63.48, 57.72, 51.54, 38.30, 36.99, 30.04, 28.88. (Figure S53-S54)

Synthesis of Compound 10 (PSF). Compound **9** (470 mg) and $CuSO_4 \cdot 5H_2O$ (7 mg, 0.028 mmol) were added to a 50 mL round-bottomed flask, then 5 mL of pure water and 5 mL of tert-butanol to the round-bottomed flask were added. Stirred until the solution was clear, then Compound **7** (210 mg, 0.24 mmol) and sodium ascorbate (80 mg, 0.24 mmol) were added and continued to react at room temperature overnight. After the reaction was completed, 20 mL of pure water was added, and the molecular weight cut-off Mw = 5000 dialysis bag was used for dialysis for 48 hours (water was replaced at the 4, 8, 16, 24, and 36 h, respectively). When the dialysis was completed, the liquid in the dialysis bag was collected and lyophilized to obtain a light green solid powder (360 mg, 52.9% yield).

^{1}H NMR (500 MHz, DMSO-d6) δ 8.56 (s, 1H), 8.35 (d, *J* = 13.8 Hz, 3H), 8.07 (s, 5H), 7.80 (d, *J* = 8.2 Hz, 3H), 7.73 (d, *J* = 8.3 Hz, 3H), 6.71 (d, *J* = 13.8 Hz, 2H), 5.14 (s, 2H), 4.48 (s, 6H), 4.19 – 4.05 (m, 10H), 3.51 (s, 819H), 3.33 (s, 81H), 3.24 (s, 15H), 2.76 (dd, *J* = 16.3, 10.4 Hz, 10H), 2.64 (s, 9H), 2.35 (d, *J* = 5.0 Hz, 5H), 2.07 (s, 6H), 1.73 (d, *J* = 5.3 Hz, 20H). ^{13}C NMR (126 MHz, DMSO-d6) δ 173.76, 172.81, 171.79, 166.34, 149.46, 145.79, 145.66, 142.52, 126.91, 126.40, 126.01, 125.73, 125.48, 123.90, 120.36, 112.50, 103.68, 72.82, 71.75, 70.25, 70.06, 68.72, 63.86,

63.76, 58.52, 49.60, 38.70, 38.59, 38.54, 37.62, 37.28, 30.33, 29.48, 27.75, 24.09. ^{19}F NMR (471 MHz, DMSO-d6) δ -59.63 (s). (Figure S55-S57)

Synthesis of Compound 11. 3-(Tritylthio)propionic acid (7.0 g, 20 mmol) was dissolved in anhydrous DMF (50 mL), and the reaction mixture was brought to 0°C. O-(Benzotriazol-1-yl)-N,N,N',N'-tetramethyluronium tetrafluoroborate (TBTU) (6.4 g, 20 mmol) was added to this solution, followed by N,N-diisopropylethyl amine (6.5 g, 50 mmol). After 0.5 h, gemcitabine (5.3 g, 20 mmol) was added and stirred for another 0.5 h at 0°C. The reaction mixture was then allowed to warm to room temperature and stirred for 18 h. The solvents were evaporated under reduced pressure, and the crude product was purified by flash chromatography, using 0–4% methanol as a gradient in dichloromethane, to obtain pure 11 as a white solid (5.4 g, 45.2% yield).

^{1}H NMR (500 MHz, CD_3OD) δ 7.54 (d, *J* = 7.6 Hz, 1H), 7.41 (d, *J* = 8.2 Hz, 6H), 7.29 (dd, *J* = 8.1, 7.3 Hz, 6H), 7.22 (dd, *J* = 10.5, 4.1 Hz, 3H), 6.24 (t, *J* = 8.0 Hz, 1H), 5.86 (d, *J* = 7.5 Hz, 1H), 4.41 (d, *J* = 3.8 Hz, 2H), 4.23 – 4.13 (m, 1H), 4.12 – 4.04 (m, 1H), 2.48 (t, *J* = 6.9 Hz, 2H), 2.28 (dd, *J* = 13.8, 6.8 Hz, 2H). ^{13}C NMR (126 MHz, CD_3OD) δ 171.52, 166.21, 156.33, 144.61, 129.33, 127.59, 126.49, 95.26, 78.49, 71.24, 69.95, 66.65, 62.11, 32.94, 26.61. ^{19}F NMR (471 MHz, CD_3OD) δ -118.30 (d, *J* = 239.2 Hz), -120.55 (d, *J* = 238.0 Hz).

HRMS (ESI) calc for $C_{31}H_{29}F_2N_3O_5S$ $[M+Na]^+$ = 616.1688, found 616.1708 (Figure S58-S61).

Synthesis of Compound 12. The compound **10** (3.4 g, 4 mmol) was added to 20 mL of TFA: CH_2Cl_2 (1: 1 ratio), followed by triethylsilane (1.2 g, 10 mmol) at 0°C, then the resulting solution was stirred for 1 h. The solvents were then removed under reduced pressure to obtain an oil, which was washed with diethyl ether (2x5 mL) and dried under reduced pressure to obtain the thiol **12** as a solid (1.3 g, 92.4% yield), which was used for the following reaction without further purification. ^{1}H NMR (500 MHz, CD_3OD) δ 8.04 (d, *J* = 7.7 Hz, 1H), 6.32 (t, *J* = 8.3 Hz, 1H), 6.11 (d, *J* = 7.8 Hz, 1H), 5.59 – 5.42 (m, 1H), 4.31 – 4.20 (m, 1H), 3.96 (dd, *J* = 12.8, 2.3 Hz, 1H), 3.81 (dd, *J* = 12.8, 3.3 Hz, 1H), 2.90 – 2.73 (m, 4H). ^{13}C NMR (126 MHz, CD_3OD) δ 170.30, 142.62, 123.48, 121.39, 119.31, 95.25, 79.94, 69.77, 59.20, 53.93, 37.72, 18.72. ^{19}F NMR (471 MHz, CD_3OD) δ -115.90 (d, *J* = 234.1 Hz), -118.17 (d, *J* = 247.1 Hz). HRMS (ESI) calc for $C_{12}H_{15}F_2N_3O_5S$ $[M+H]^+$

= 352.0773, found 352.0787 (Figure S62-S65).

Synthesis of Compound 13. The thiol **12** (1.2 g, 3.4 mmol) and 2, 2'-dithiodipyridine (1.5 g, 6.8 mmol) were dissolved in anhydrous methanol (20 mL) containing glacial acetic acid (100 μL, 1 mmol). The reaction mixture was stirred at room temperature for 18 h, and the solvent was removed under reduced pressure to obtain the crude product. The crude product was purified by flash chromatography (using a 0–7% methanol gradient in dichloromethane) to obtain compound **13** as a white solid (0.6 g, 40.2% yield).

^{1}H NMR (500 MHz, CD_3OD) δ 8.44 – 8.35 (m, 1H), 7.88 – 7.75 (m, 2H), 7.58 (d, *J* = 7.6 Hz, 1H), 7.22 (ddd, *J* = 6.7, 4.9, 1.8 Hz, 1H), 6.25 (t, *J* = 8.4 Hz, 1H), 5.96 (d, *J* = 7.6 Hz, 1H), 4.47 (ddd, *J* = 17.4, 12.5, 3.9 Hz, 2H), 4.22 (dd, *J* = 18.8, 10.8 Hz, 1H), 4.12 (ddd, *J* = 7.8, 4.9, 2.9 Hz, 1H), 3.10 (t, *J* = 6.8 Hz, 2H), 2.86 (t, *J* = 6.7 Hz, 2H). ^{13}C NMR (126 MHz, CD_3OD) δ 171.23, 166.19, 159.54, 156.29, 149.11, 137.82, 121.12, 119.99, 95.33, 79.37, 77.77, 71.23, 69.35, 62.45, 54.45, 53.46, 33.14. ^{19}F NMR (471 MHz, CD_3OD) δ -118.49 (d, *J* = 238.6 Hz), -120.50 (d, *J* = 224.6 Hz). HRMS (ESI) calcd for $C_{17}H_{19}N_4O_5F_2S_2$ $[M+H]^+$ = 461.0759, found 461.0808. (Figure S66-S69).

Synthesis of Compound 14 (PSG). An oven-dried 25 mL flask with a magnetic stir bar was charged with mPEG-SH (MW = 1000, 1.0 g, 1 mmol) and gemcitabine dithiopyridine **13** (0.9 g, 2 mmol) under a nitrogen atmosphere. Anhydrous DMF (20 mL) was added to this mixture, followed by triethylamine (200 μL, 1 mmol), and stirred at room temperature overnight. The solvent was removed under reduced pressure, and the resulting residue was purified by silica gel flash chromatography using a gradient of 10−15% methanol in dichloromethane containing 0.1% triethylamine. PSG was obtained as a pale yellow solid (0.5 g, 0.38 mmol) in 38.2% yield.

^{1}H NMR (500 MHz, CD_3OD) δ 7.84 (d, *J* = 7.4 Hz, 1H), 7.62 (d, *J* = 7.6 Hz, 1H), 6.28 (dt, *J* = 16.5, 8.5 Hz, 2H), 5.98 (dd, *J* = 14.3, 7.6 Hz, 1H), 5.53 – 5.40 (m, 1H), 4.47 (ddd, *J* = 17.5, 12.4, 3.9 Hz, 2H), 4.27 – 4.06 (m, 2H), 3.94 (dd, *J* = 12.8, 2.4 Hz, 1H), 3.86 – 3.70 (m, 3H), 3.63 (d, *J* = 9.5 Hz, 82H), 3.36 (s, 2H), 3.07 – 2.97 (m, 2H), 2.96 – 2.88 (m, 3H), 2.86 (dd, *J* = 13.4, 6.7 Hz, 2H), 1.46 – 1.32 (m, 2H). ^{13}C NMR (126 MHz, CD_3OD) δ 171.54, 170.37, 166.12, 156.05, 95.16, 71.58, 70.95, 69.35, 68.99, 57.71, 54.45, 38.27, 32.90, 17.31, 15.87. ^{19}F NMR (471 MHz, CD_3OD) δ -117.92 – -

120.35 (m). (Figure S70-S72)

3. Characterization of Co-assembly Polymeric Micelles.

Drug loading content (DLC) and drug loading efficiency (DLE) of GEM were measured via ^{19}F NMR spectrum and HPLC (samples were pretreated with 10 mM GSH for 24 h) at 268 nm (MeOH: Water = 85: 15, v: v) and were calculated by using Equation (1) and Equation (2), respectively.

$$\mathrm{DLC}(\%) = \frac{\text{Weight of GEM in prodrug micelles}}{\text{Weight of prodrug micelles}} \times 100 \quad (1)$$

$$\mathrm{DLE}(\%) = \frac{\text{Weight of PSG in prodrug micelles}}{\text{Initial feeding amount of PSG}} \times 100 \quad (2)$$

The critical micelle concentration (CMC) of the copolymer was measured by a fluorescence spectrometer (FS5) using pyrene as a fluorescence probe. Briefly, 100 μL of a pyrene solution in acetone (~6 μM) was added into a test tube. When acetone was evaporated, 2 mL of an aqueous PSFG NPs solution ranging from 1.0 μg·mL^{-1} to 0.5 mg·mL^{-1} was added to the test tube separately. After sonication for 5 min, the mixture was kept at room temperature for 24 h to allow pyrene to equilibrate in the aqueous phase. Fluorescence spectra were recorded on an FS5 luminescence spectrometer with an excitation wavelength of 330 nm. The emission wavelengths were recorded ranging from 350 nm to 500 nm. The CMC value was estimated as the cross-point of the intensity of I_{397} to the micelles concentration.

Redox Sensitive Behavior: The redox-sensitive behavior of micelles in PBS solution in the presence of a high level of GSH was evaluated by fluorescence emission spectrum. At the selected time or GSH conclusion intervals, the fluorescence intensity of the solution was measured. In addition, the morphology of micelles was further investigated by TEM after incubation with different concentrations of GSH for 8 h.

Fluorescence Behavior of Prodrug Micelles: It is commonly accepted that Cy7 is a typical ACQ fluorescent probe. Here, the fluorine-containing groups introduced into the newly designed and synthesized FCy7 do not affect its basic fluorescence properties. That is, FCy7 is also considered an ACQ probe. The ACQ behavior of prodrug micelles was evaluated by fluorescence spectra. Typically, a series of solutions with the same concentration of prodrug micelles and different

volume ratios of H_2O and DMSO were prepared to determine the fluorescence intensity. Moreover, the GSH-induced fluorescence turn-on behavior was also studied by incubating polymeric micelles with 200 μM GSH, and the fluorescence intensity was monitored over time.

4. Biocompatibility and Cytotoxicity.

The biocompatibility and cytotoxicity of the PSFG were assessed by performing standard methyltetrazolium (MTT) viability assays with the A549 cells, as described previously. The cells were seeded in 96-well plates at a density of 1×10^4 cells per well in 100 μL complete F12K and incubated at 37°C in 5% CO_2 atmosphere for 24 h. After removing the culture medium, PSFG micelles diluted in complete F12K (100 μL) were added to cell wells with various concentrations of PSFG from 0 to 100 μg mL^{-1}. The cells were incubated for another 12 h. After the incubation, the culture medium was removed, and the cells were washed with PBS three times. Then 200 μL of F12K and 20 μL of 5 mg mL^{-1} MTT assays stock solution in PBS were added. After incubating the cells for 4 h, the unreacted MTT medium was removed carefully. The obtained blue formazan crystals were dissolved in 200 μL per well DMSO. The absorbance of the solution was measured on an enzyme-linked immunosorbent assay (Elisa) at 490 nm. Cell viability (%) was calculated based on the following equation: $(A_{sample}/A_{control}) \times 100\%$, where A_{sample} and $A_{control}$ denote as absorbencies of the sample well and control well, respectively.

Hemolysis Test: Whole blood from rats was collected in centrifuge tubes, 3 mL of blood was taken out and centrifuged at 4000 rpm for 5 min to separate the various organelles. Then the lowest layer of red blood cells was diluted with PBS (pH 7.4) in 10-fold dilution. Polymeric micelles with different concentrations were prepared in the PBS buffer and added to the diluted solution with the same concentration of red blood cells. The negative control with PBS and the positive control with deionized water without polymeric micelles was added. After incubation at room temperature for 2 h, the solutions were centrifuged at 1000 rpm for 5 min, then 100 μL supernatant was removed into 96-well plates, and the release of hemoglobin was determined by photometric analysis at 541 nm. Less than 5% hemolysis was regarded as suitable in the experiments.

5. Animals and Cancer Model Mice.

All experimental protocols involving animals were approved by the Animal Welfare and Research Ethics Committee at the Innovation Academy for Precision Measurement Science and Technology, Chinese Academy of Sciences (APM23024T). All BALB/c male nude mice (5-6 weeks of age, approximately 18-20 g) were purchased from Beijing Vital River Laboratory Animal Technology Co. Ltd. and fed on SPF grad mice feed. *In situ* lung cancer model mice were produced according to related reports. Briefly, about 1×10^6 A549 cells in 0.5 mL F12K culture medium were mixed with an equal volume of matrix glue. When the left lung was cut open, 50 μL cell gel was injected into the left lung of nude mice. After surgery, the physiological health status of nude mice was monitored to avoid infection. In addition, the tumor size was monitored by CT and ^{1}H MRI every week.

A549 tumor-bearing mice (BALB/c, male, 18-20 g) were fed to estimate GEM prodrug micelles' antitumor ability. A549 suspension cells were used to establish the animal xenograft tumor model by injecting subcutaneously at the density of 1×10^6 A549 cells per mouse. The mice were divided into five groups equally (n = 6). When the tumor volume reached about 100 mm^3, PBS, PSF, GEM, PSG, and prodrug micelles PSFG were injected by subcutaneous injection every 3 days, and the body weight of the mice and tumor volume was measured every 3 days. At the end of the experiment, all mice were sacrificed, and the major organs (heart, liver, spleen, lung, and kidney) and tumors were harvested. These tissues were washed with PBS, fixed with 4% paraformaldehyde solution, dehydrated, embedded in paraffin, sliced about 4 μm thick, stained with H&E staining, observed and described after panoramic scanner scanning. In addition, CD31, Ki67, and TUNEL were measured for analyzing the tumor's cell proliferation and tumor suppression ability.

6. *Ex Vivo* Fluorescence Imaging.

In order to investigate the metabolism and accumulation ability of GEM prodrug polymeric micelles in tumor sites, the tumors and major organs of BALB/c mice were imaged with *ex vivo* fluorescence imaging using a PerkinElmer Co. Ltd Living Imaging System. Typically, the mice were injected with GEM prodrug micelles at a dose of 5 mg GEM kg^{-1} body weight via the tail vein when the tumor volume reached about 400 mm^3. After injection for 6, 12, 24, and 48 h, the mice were sacrificed, and the major organs (heart, liver, lung, spleen, and kidney) and the tumors were taken

out and then washed with PBS three times. Finally, the tumors and organs were imaged with *ex vivo* fluorescence imaging.

7. Hematology and Histology Examinations

Ten mice were randomly assigned to two groups. PSFG NPs (500 μg) were intravenously injected (via tail vein) into the mice as the test group. The other mice were administered an injection of saline and selected as the control group. The mice were sacrificed on day 7 post-injection. Blood was collected from the orbital sinus by quickly removing the eyeball from the socket with a pair of tissue forceps. Blood routine indexes (white blood cells (WBC), red blood cells (RBC), hemoglobin (HGB), hematocrit (HCT), mean corpuscular volume (MCV), mean corpuscular hemoglobin (MCH), mean corpuscular hemoglobin concentration (MCHC), red cell distribution width (RDW), platelet (PLT), plateletcrit (PCT), mean platelet volume (MPV), platelet distribution width (PDW), lymphocyte count (LY), lymphocyte ratio (LYM), monocytes (MO), neutrophil count (NEUT), neutrophil ratio (NEUTR)) were tested. The mice's organs were excised, fixed in 4% paraformaldehyde solution, and embedded in paraffin. They were then sectioned and stained with hematoxylin and eosin. The histological sections were tested for *in vivo* toxicity.

Table S1. Particle size and potential energy of four different micelles.

Micelle	PSF	PSG	PSFG	PF
Size (nm)	120.8	91.7	106.3	118.4
ζ (mV)	-25.18	-12.93	-20.37	-24.56

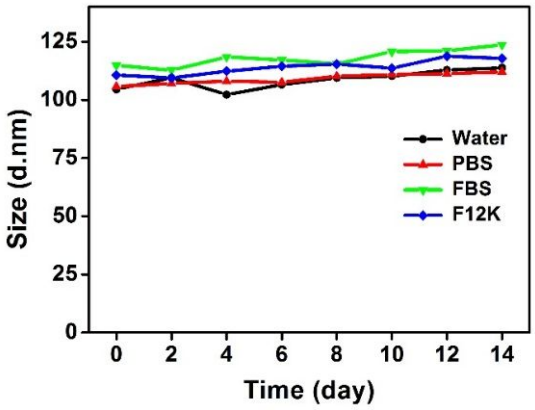

Figure S2. Particle size changes of PSFG NPs in different solvents and at different time points.

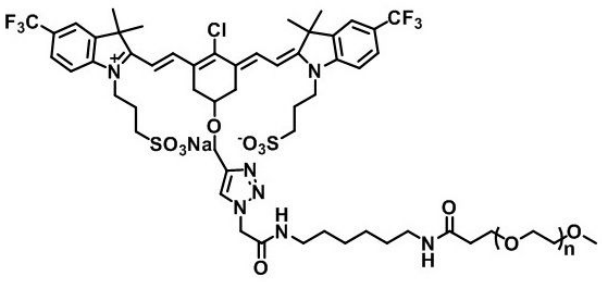

Figure S3. The chemical structure of PF.

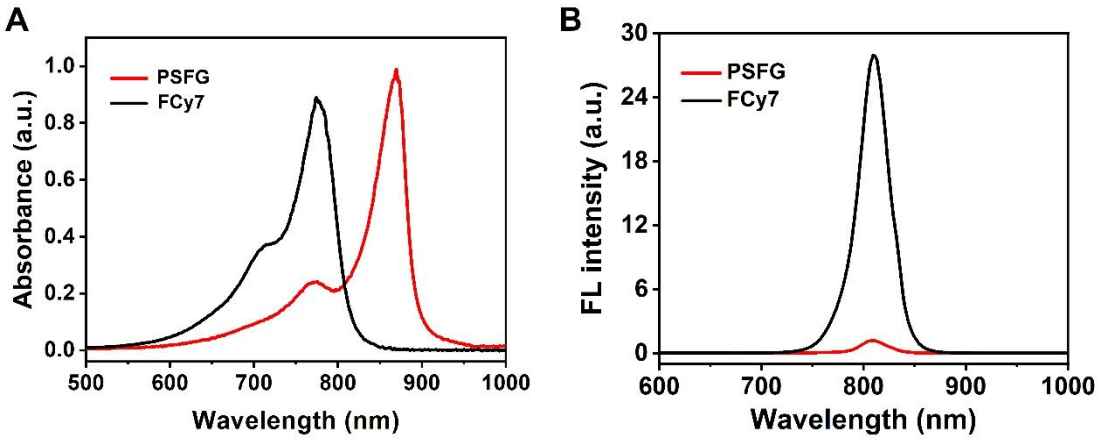

Figure S4. (A) UV-vis absorption spectra and (B) fluorescence emission spectra of PSFG (red) and FCy7 (black) in water.

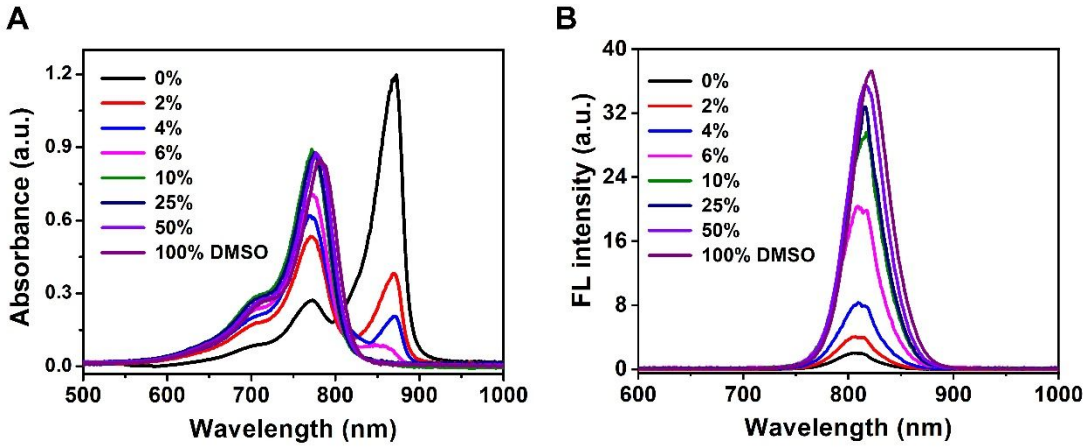

Figure S5. (A) UV-vis absorption and (B) fluorescence emission spectra in a mixed solution of H_2O and DMSO with different DMSO fractions.

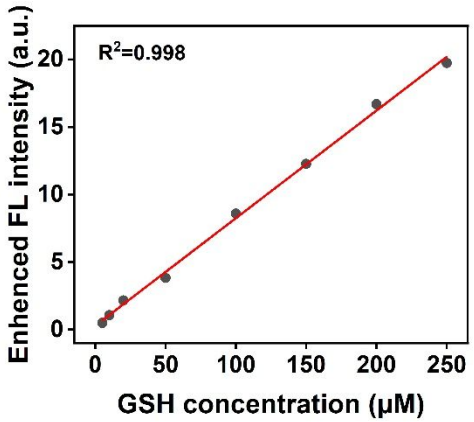

Figure S6. The maximum fluorescence intensity of PSFG micelle (10 μg mL^{-1}) was a reaction with different GSH concentrations (5-250 μM). The corresponding detection limit based on the calculation of the standard deviation was as low as 0.83 μM.

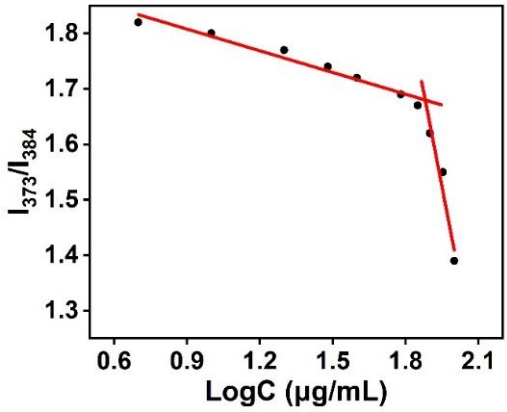

Figure S7. The CMC of PSF.

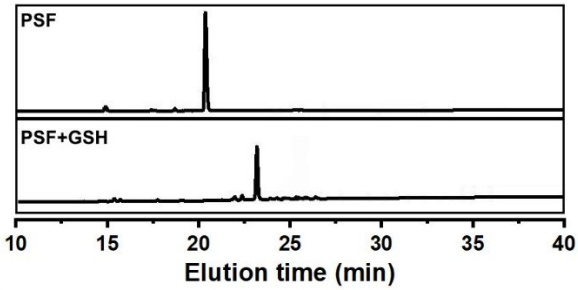

Figure S8. HPLC profiles of PSFG mixed with 10 mM GSH for 10 h.

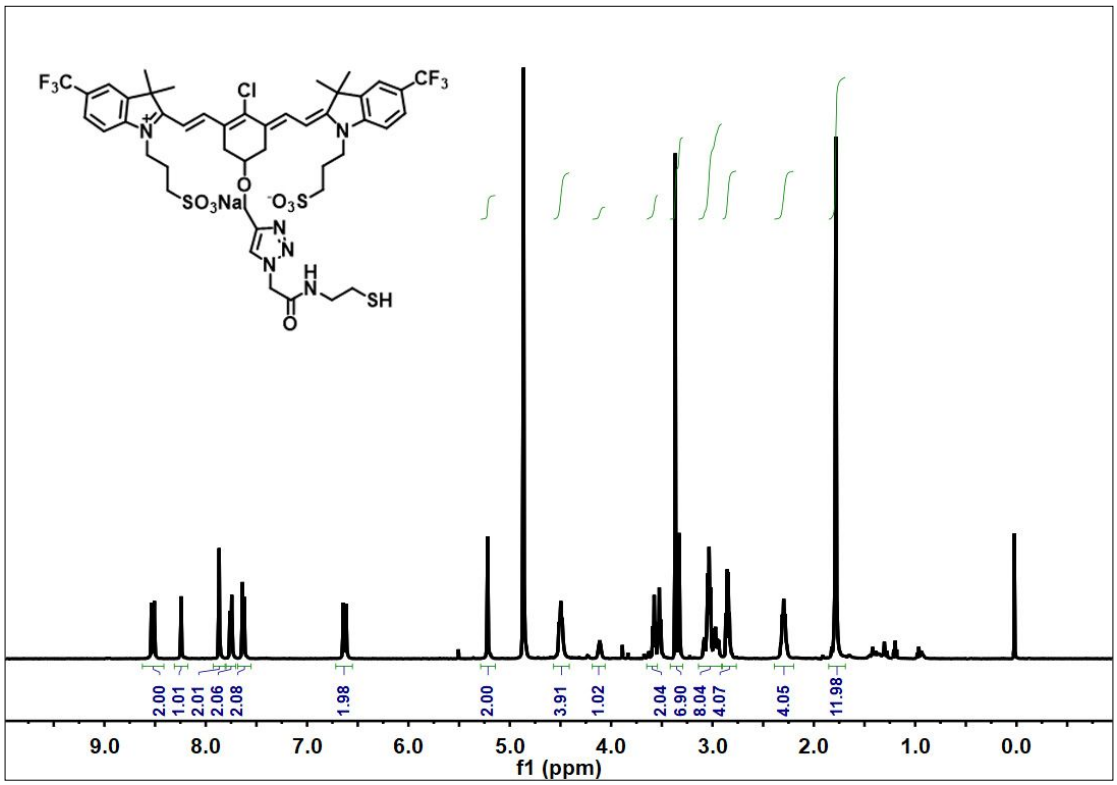

Figure S9. The ^{1}H NMR of FCy7-SH.

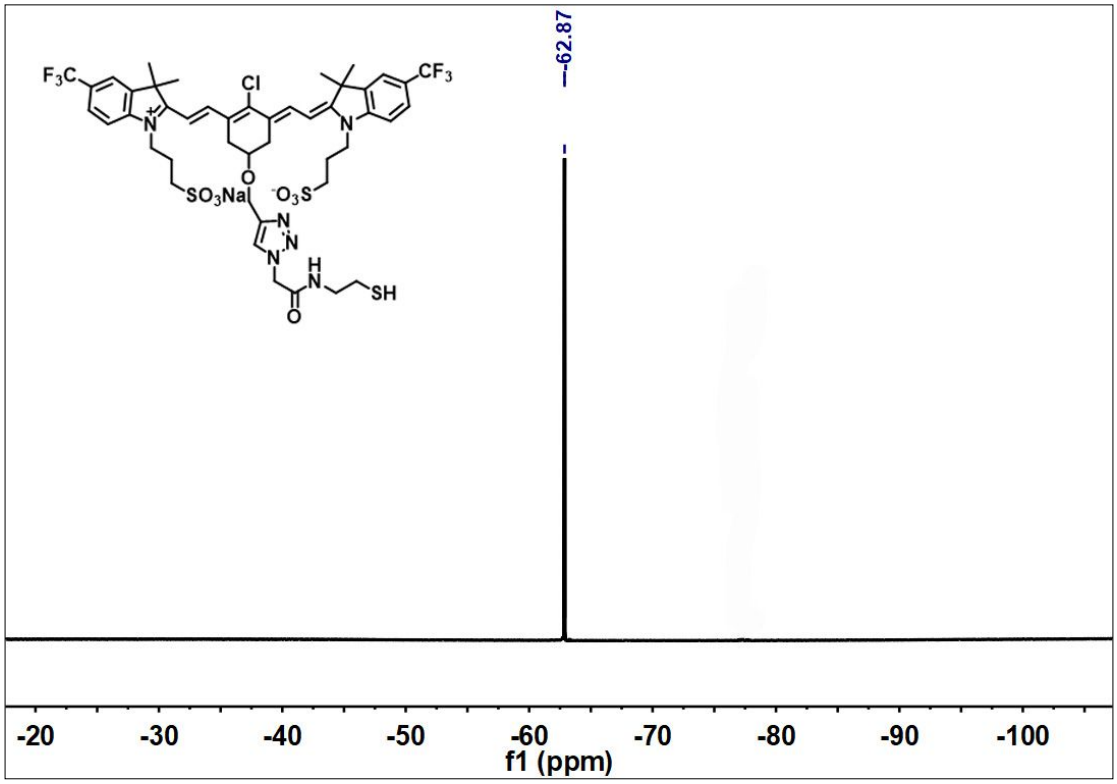

Figure S10. The ^{19}F NMR of FCy7-SH.

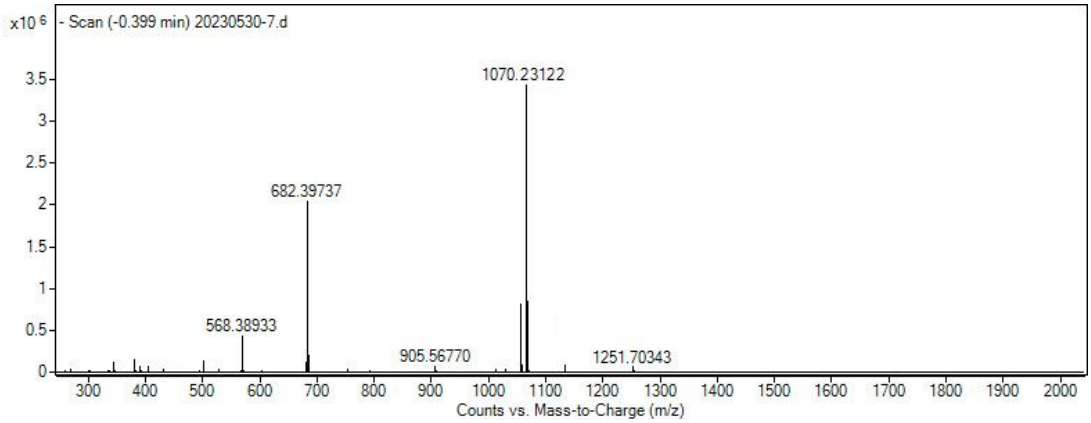

Figure S11. HRMS spectra of target compound FCy7-SH, HRMS (ESI) calcd for $C_{45}H_{50}N_6O_8S_3F_6Cl$ $[M+Na]^+$ = 1070.2337, found 1070.2312.

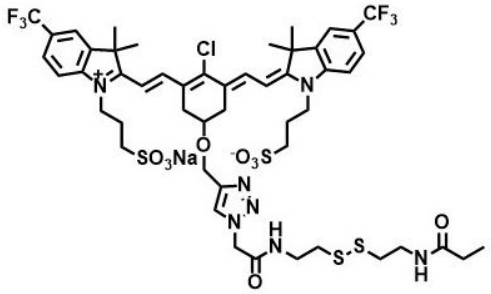

Figure S12. The chemical structure of FCy7-SS-Acetyl.

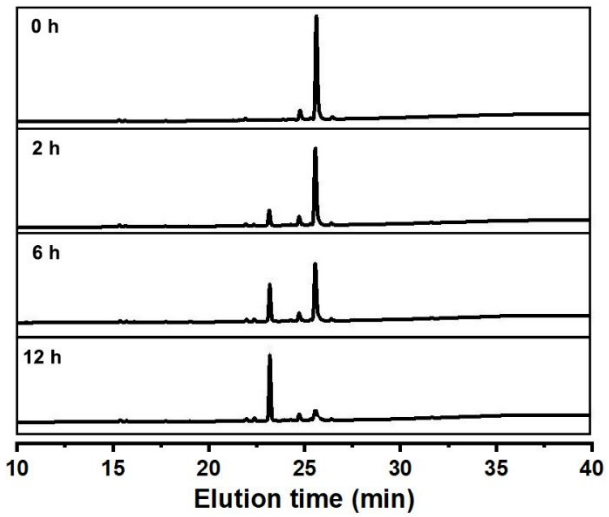

Figure S13. HPLC profiles of FCy7-SS-Acetyl mixed with 10 mM GSH.

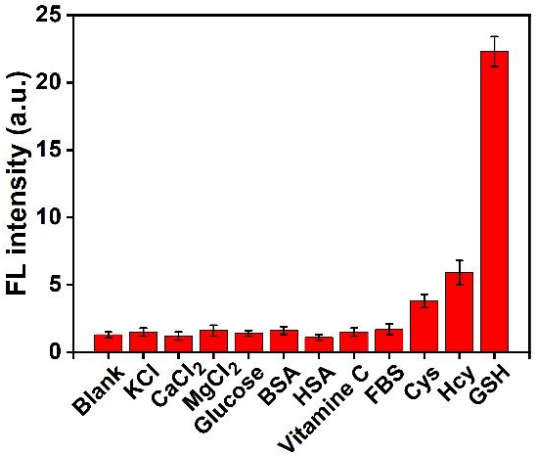

Figure S14. Fluorescence responses of PSFG to various substances: blank (PBS), KCl (1 mM), $CaCl_2$ (1 mM), $MgCl_2$ (1 mM), glucose (1 mM), BSA (1 mM), HAS (1 mM), vitamin C (1 mM), FBS (10% in PBS), Cys (1 mM), Hcy (1 mM), and GSH (1 mM). The data represent the mean and standard deviation (n = 3). $\lambda_{ex}/_{em}$ = 776/808 nm.

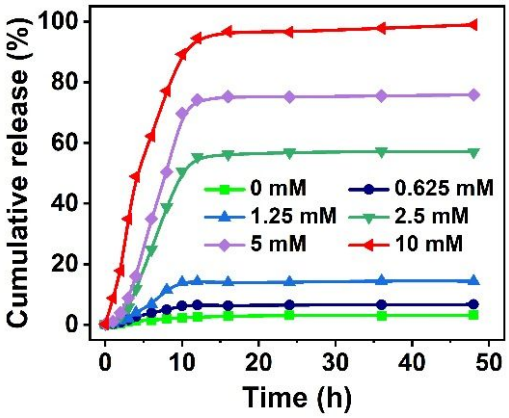

Figure S15. GSH-responsive GEM release.

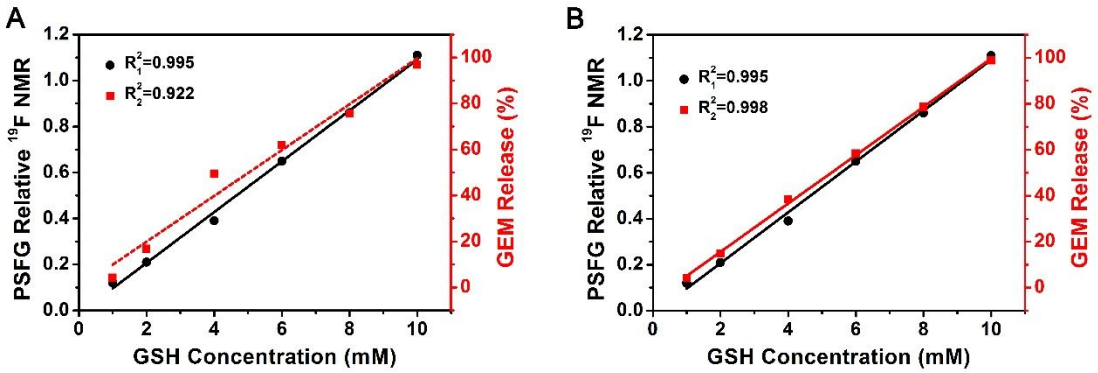

Figure S16. Detection of GEM release. (A) The fitting of the ^{19}F signal in FCy7 was compared with the ^{19}F signal in GEM by direct sampling. (B) The content of GEM detected by HPLC was compared with the reference of the ^{19}F signal in FCy7.

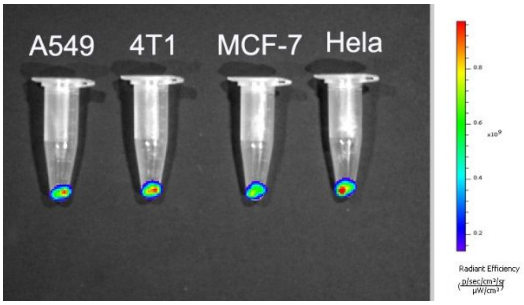

Figure S17. GSH levels in different tumor cell lines were detected by FLI.

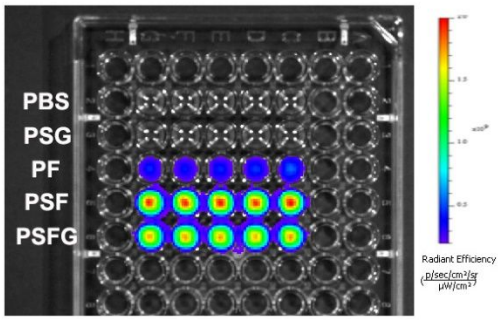

Figure S18. Fluorescence observation of different treatments after incubation with A549 cells (excitation, 745 nm; emission, 800 nm, n = 5).

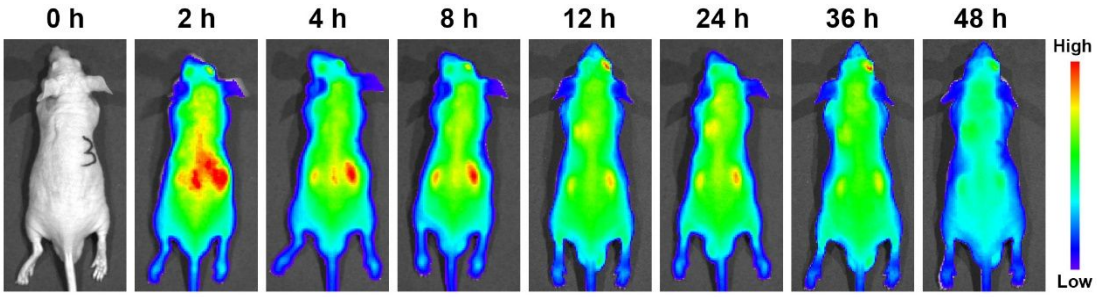

Figure S19. Observation of *in vivo* fluorescence in orthotopic lung cancer model mice at different time points after intravenous injection of PF.

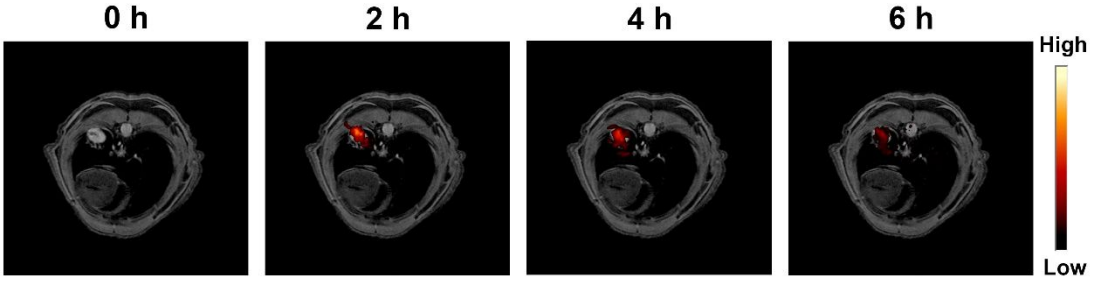

Figure S20. $^{1}H/^{19}F$ MR images of A549 *in suit* lung cancer-bearing mice after drip irrigation of PSFG micelle (10 mg/mL, 20 μL) at 2 h, 4 h, and 6 h. The same dosage of PSFG was subcutaneously injected into a normal lung for comparison. ^{1}H MRI was conducted with a T_2-weighted imaging method.

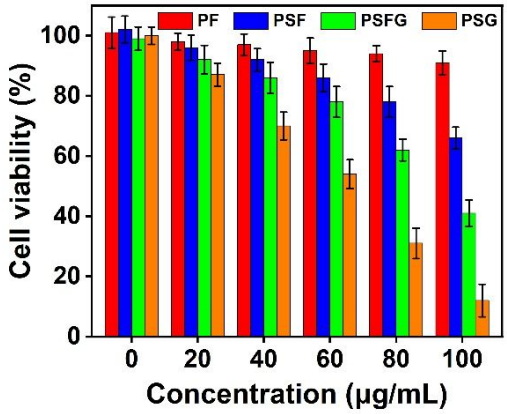

Figure S21. Cell viability of A549 cells incubated with different concentrations of PF (red), PSF (blue), PSFG (green), and PSG (orange).

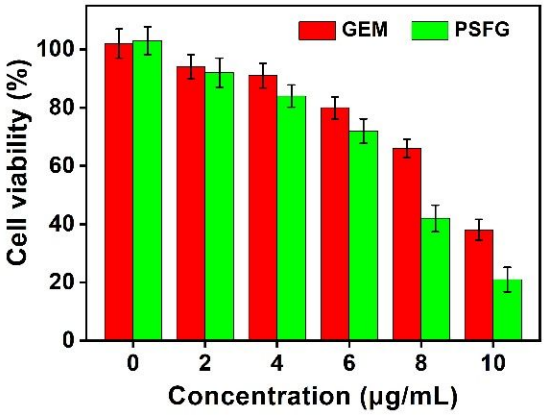

Figure S22. Cytotoxicity of free GEM at different concentrations compared to the PSFG. The PSFG was weighed in the GEM fraction contained, i.e., the drug content was guaranteed to be consistent in each group.

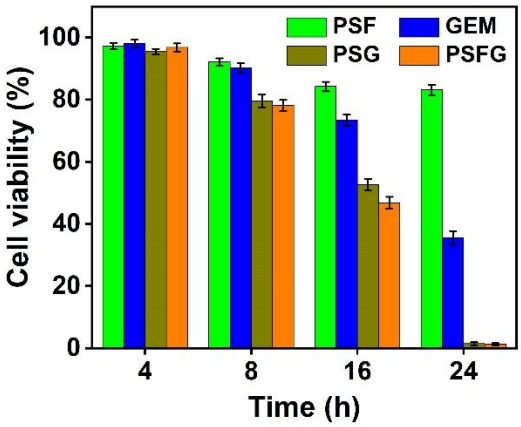

Figure S23. Rate of cellular viability for 4, 8, 16, and 24 h. PSF (green), GEM (blue), PSG (bottle green), and PSFG (orange) treatments.

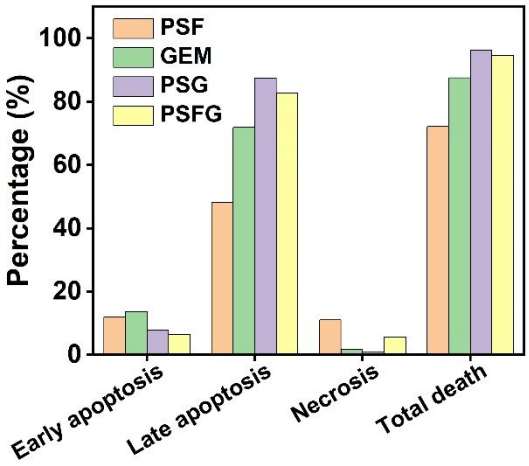

Figure S24. The statistical analysis data of cell apoptosis assay.

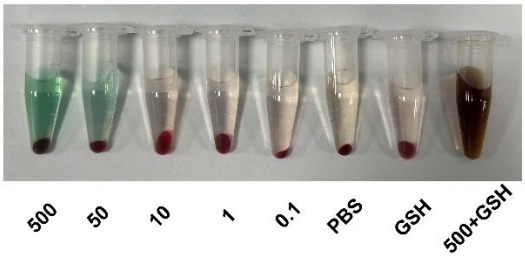

Figure S25. In the hemolysis analysis of micelles with different concentrations, the percent of hemolysis was less than 5%, even the micellar concentration up to 500 μg mL^{-1}.

Table S2. Liver and kidney functions before and 21 days after treatment

Index	Control group (n=10)		Study group (n=7)	
	Pretherapy	Treatment (21 d)	Pretherapy	Treatment (21 d)
ALT (U/L)	54.2 ± 8.8	62.4 ± 9.8	65.4 ± 8.2	70.9 ± 11.3
AST (U/L)	109.9 ± 3.1	104.2 ± 2.5	103.3 ± 2.6	110.5 ± 2.9
CRE (μmol/L)	14.2 ± 4.5	13.4 ± 4.8	15.1 ± 4.2	12.8 ± 3.8
CK (U/L)	1456 ± 410	1355 ± 387	1368 ± 422	1658 ± 398
BUN (mmol/L)	12.5 ± 2.0	15.5 ± 1.3	14.8 ± 2.8	13.9 ± 2.6

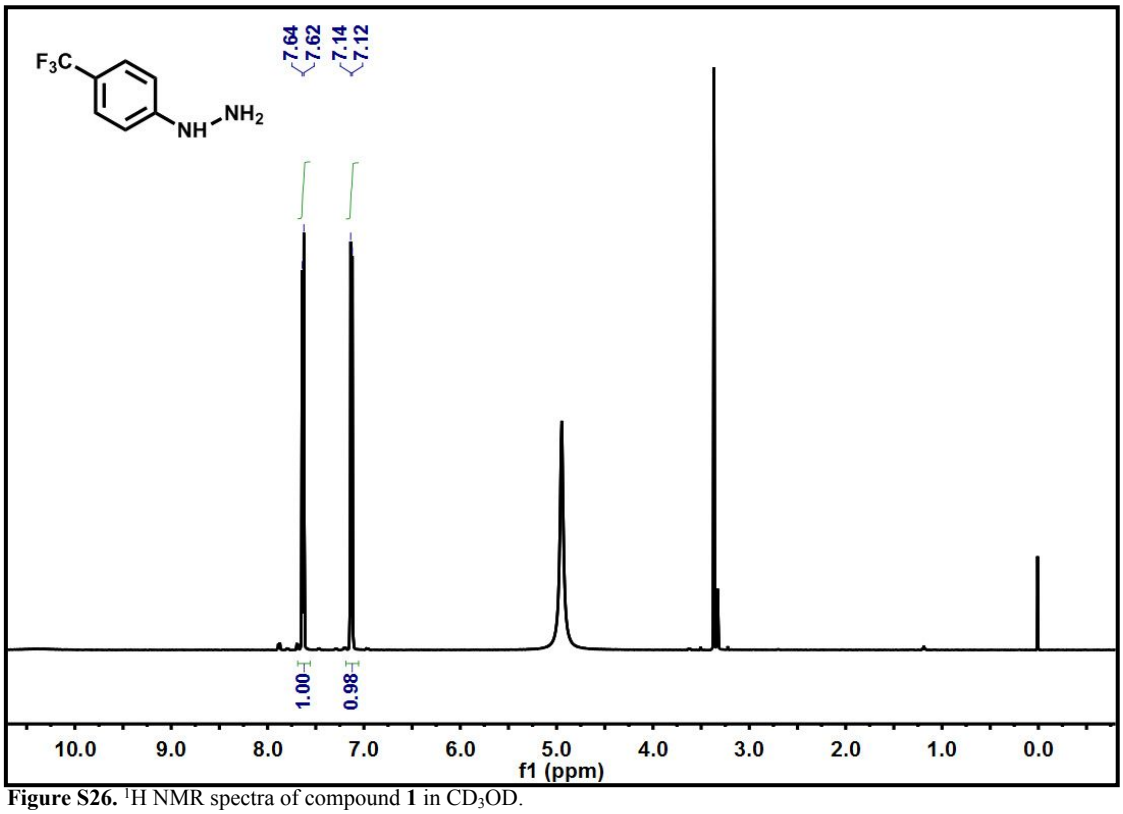

Figure S26. ^{1}H NMR spectra of compound **1** in CD_3OD.

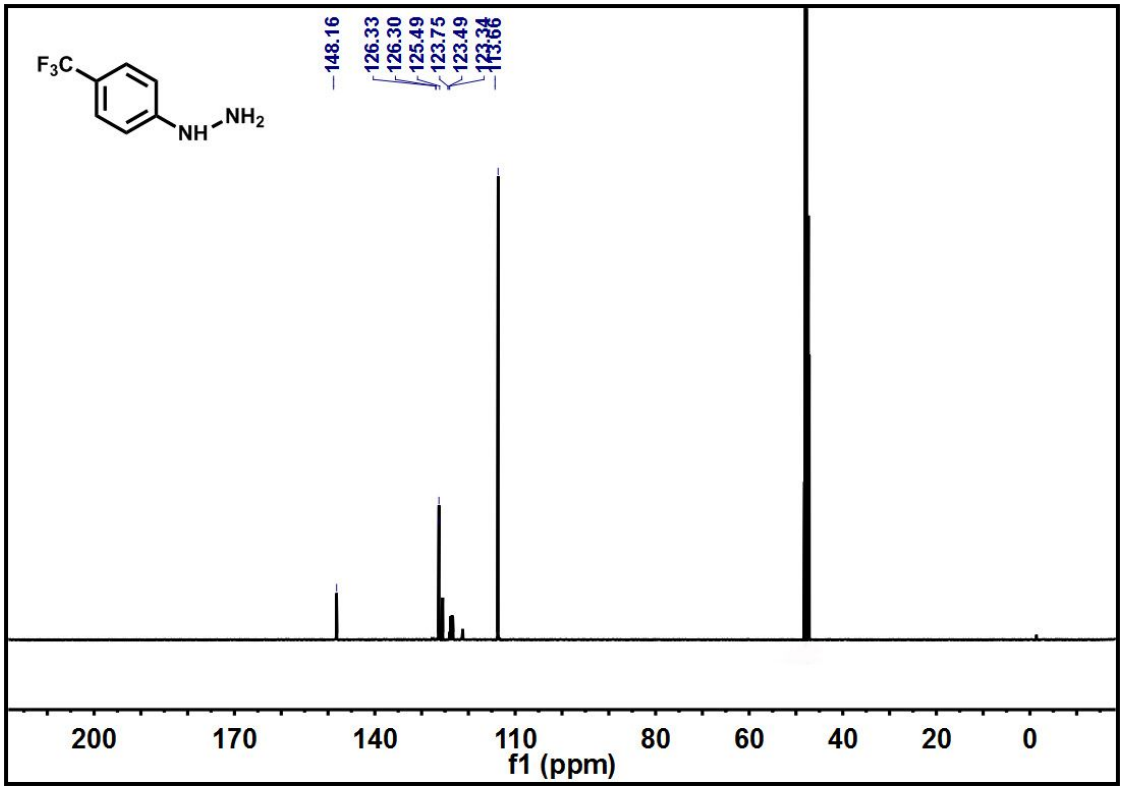

Figure S27. ^{13}C NMR spectra of compound **1** in CD_3OD.

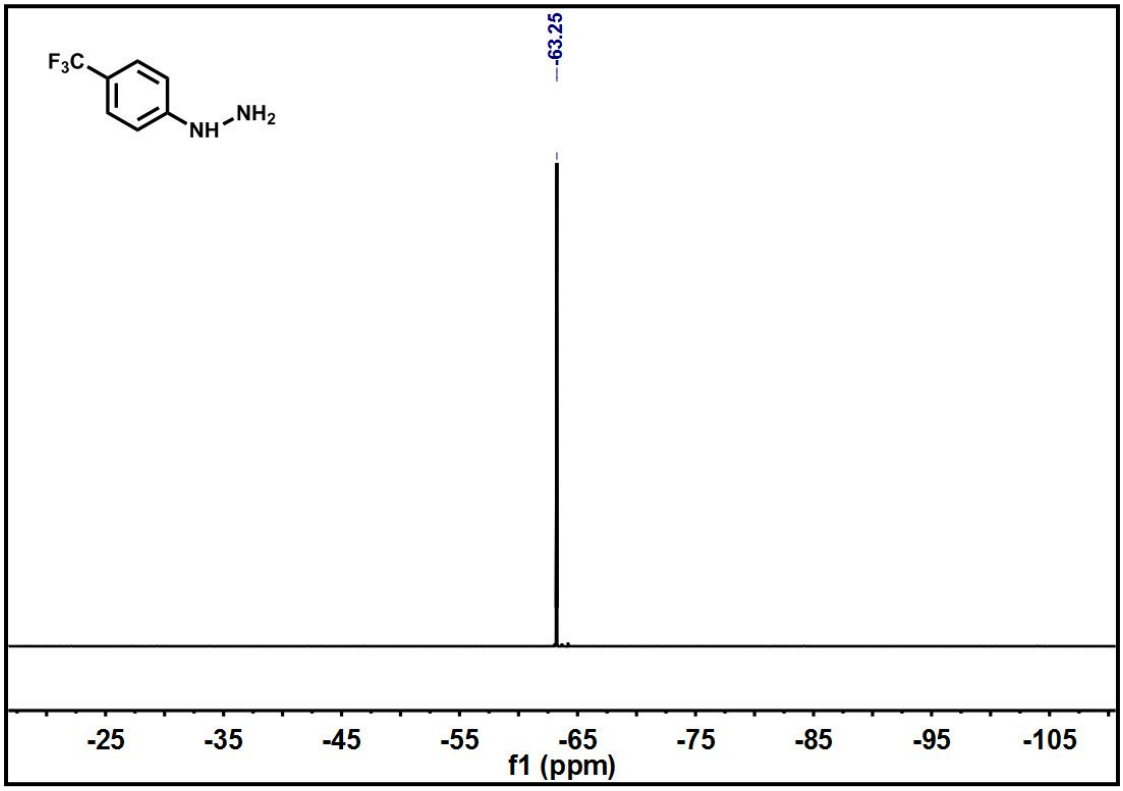

Figure S28. ^{19}F NMR spectra of compound **1** in CD_3OD.

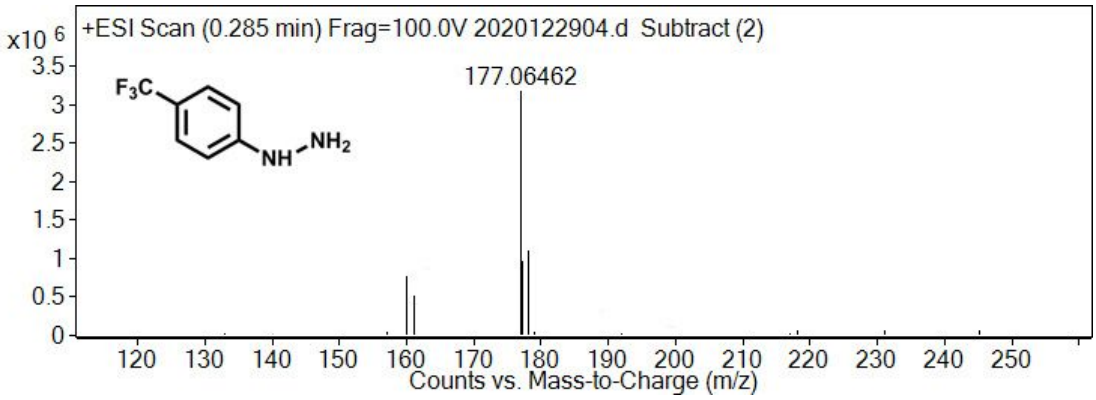

Figure S29. HRMS spectra of compound **1**.

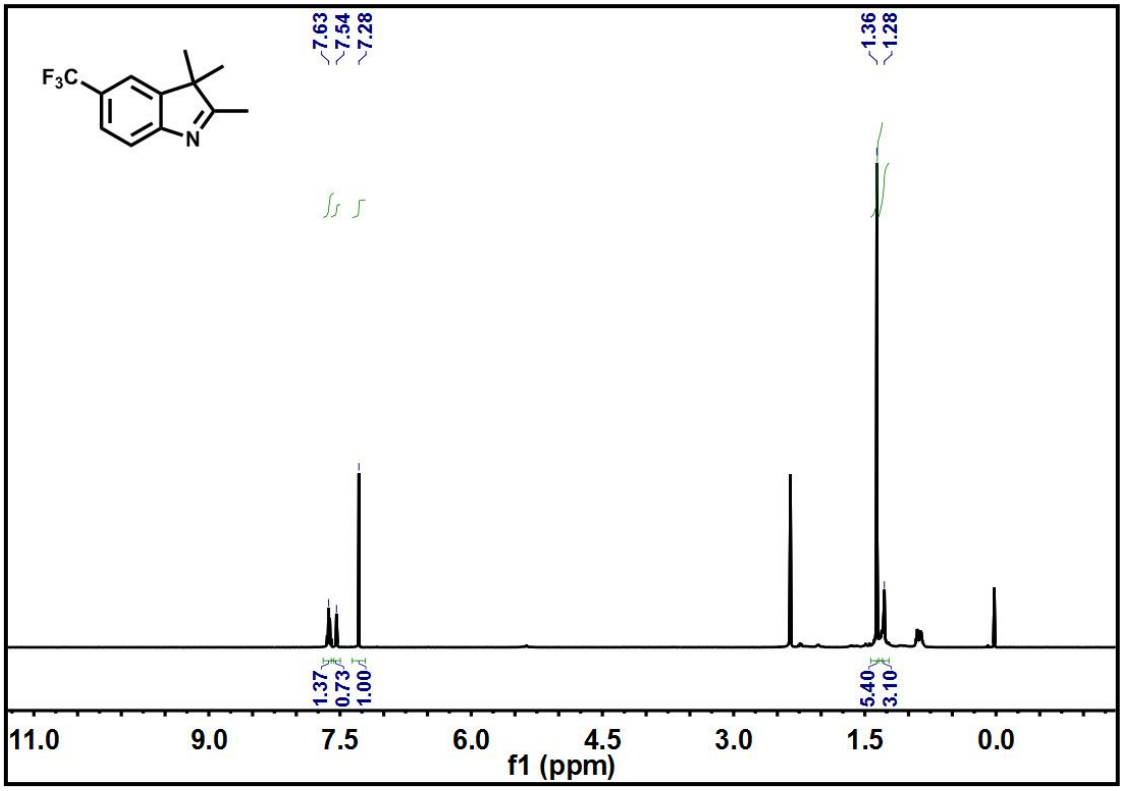

Figure S30. ^{1}H NMR spectra of compound **2** in CD_3OD.

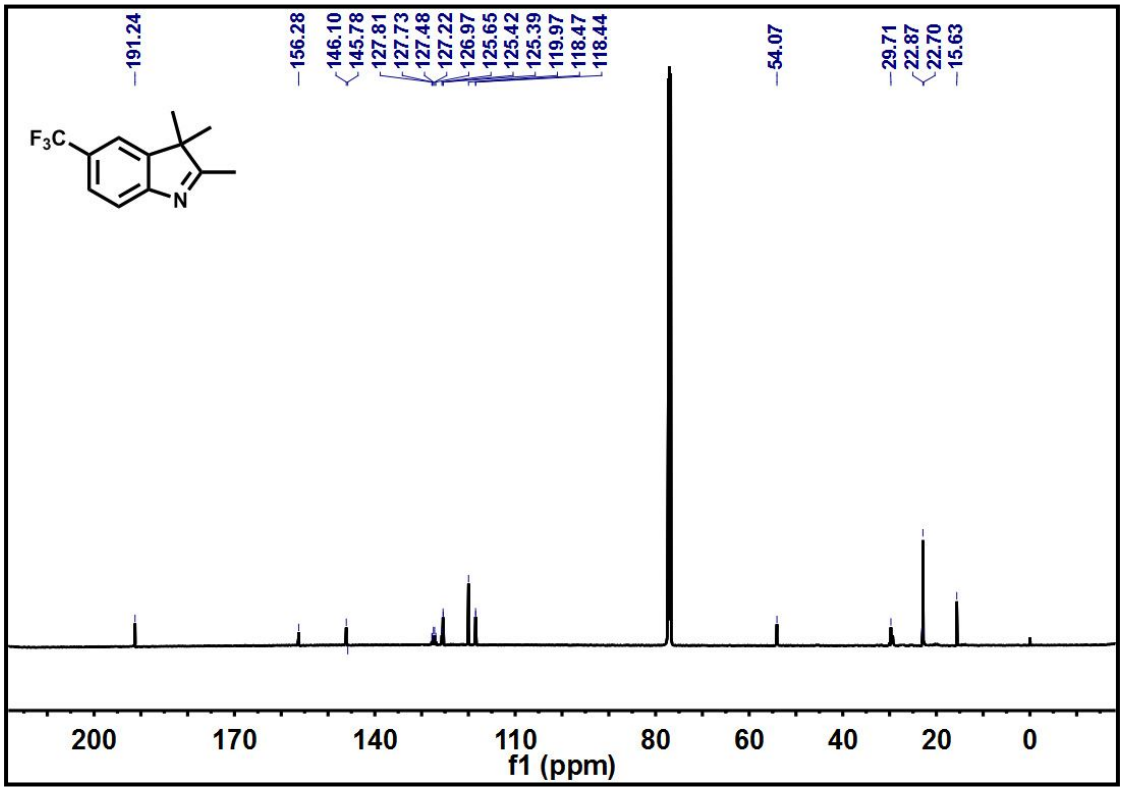

Figure S31. ^{13}C NMR spectra of compound **2** in CD_3OD.

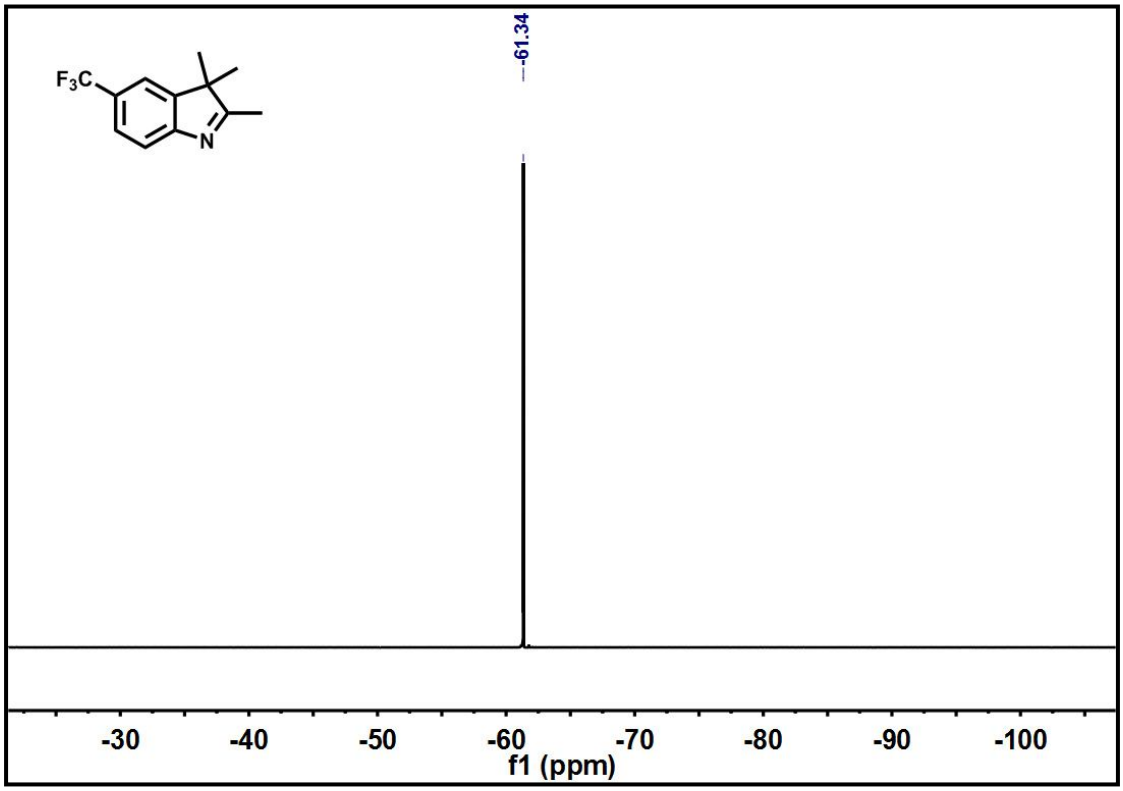

Figure S32. ^{19}F NMR spectra of compound **2** in CD_3OD.

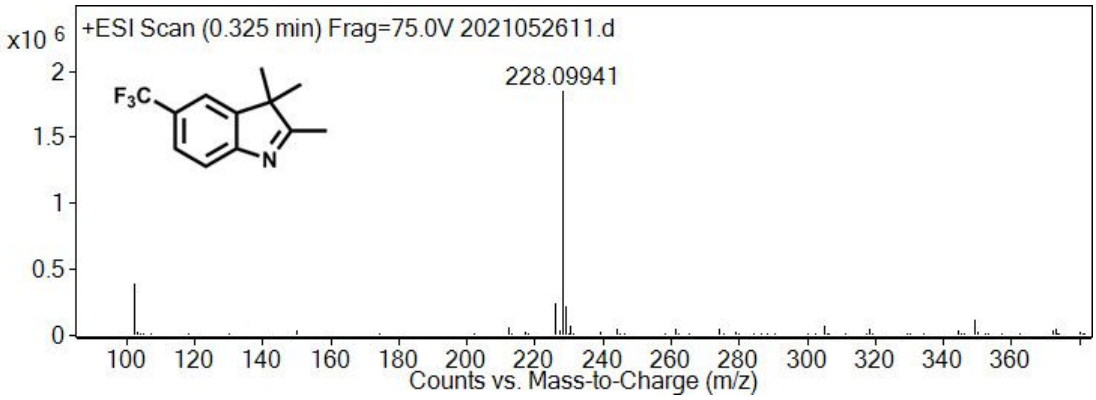

Figure S33. HRMS spectra of compound **2**.

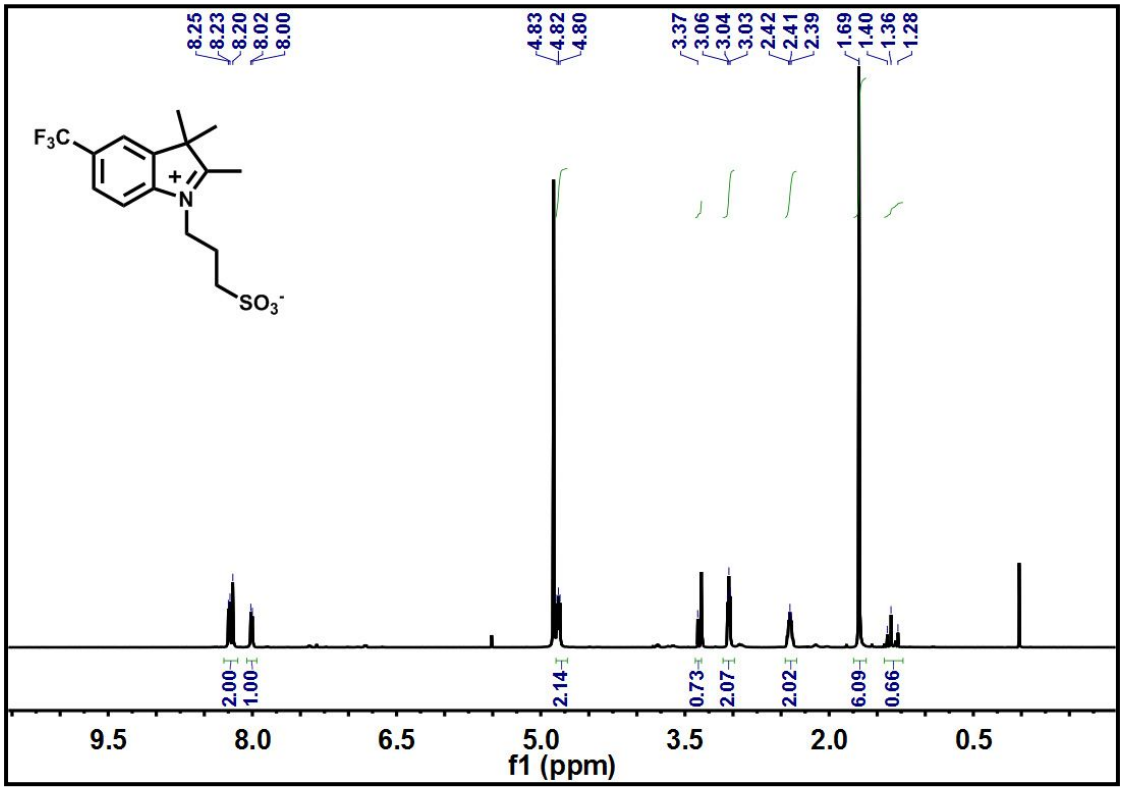

Figure S34. ^{1}H NMR spectra of compound **3** in CD_3OD.

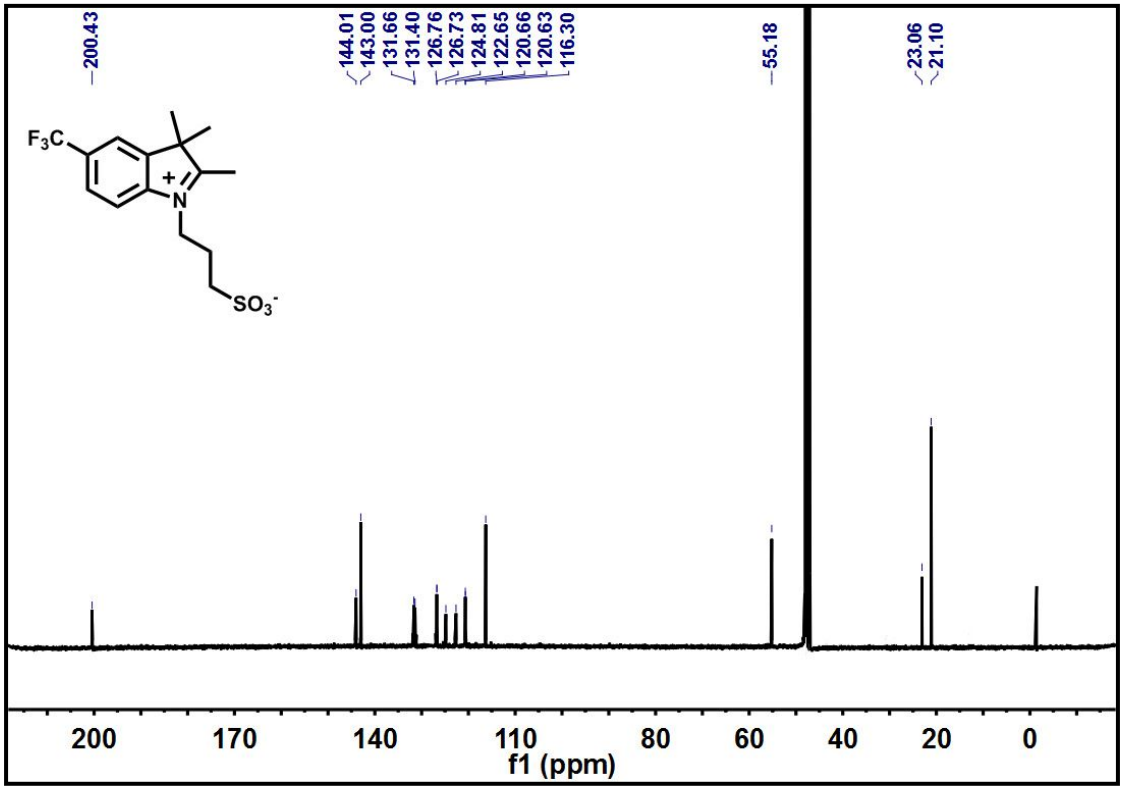

Figure S35. ^{13}C NMR spectra of compound **3** in CD_3OD.

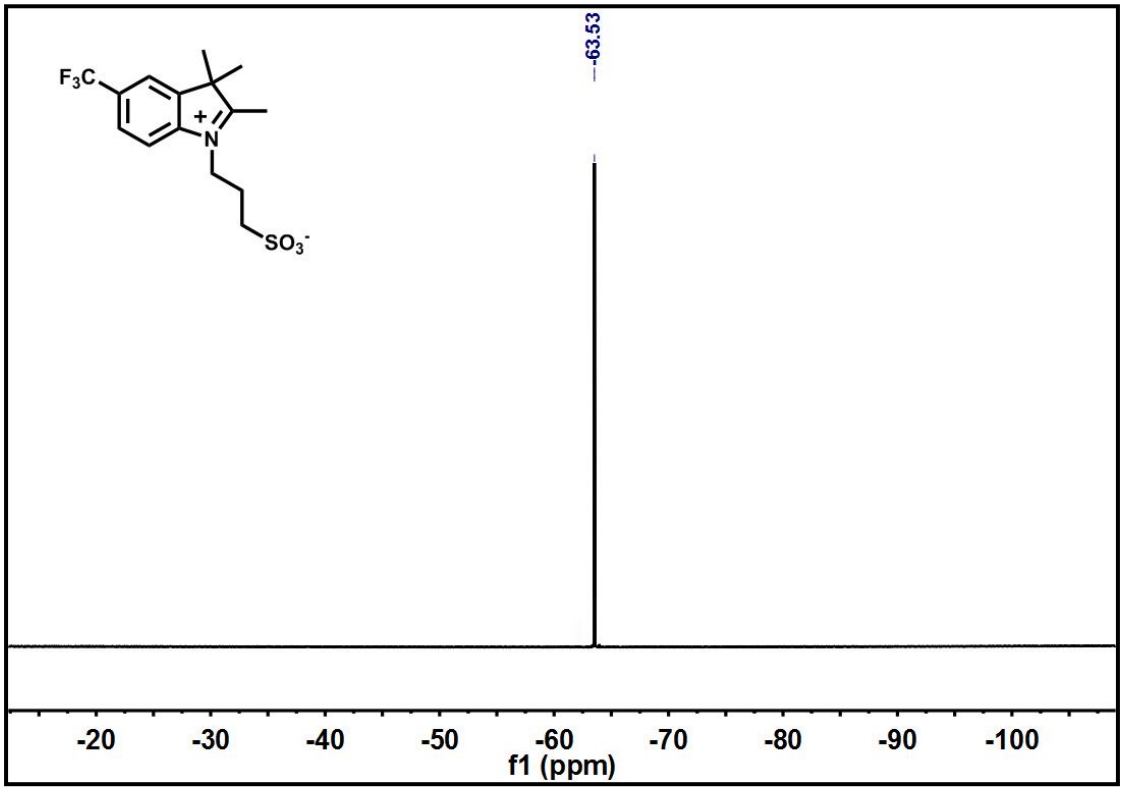

Figure S36. ^{19}F NMR spectra of compound **3** in CD_3OD.

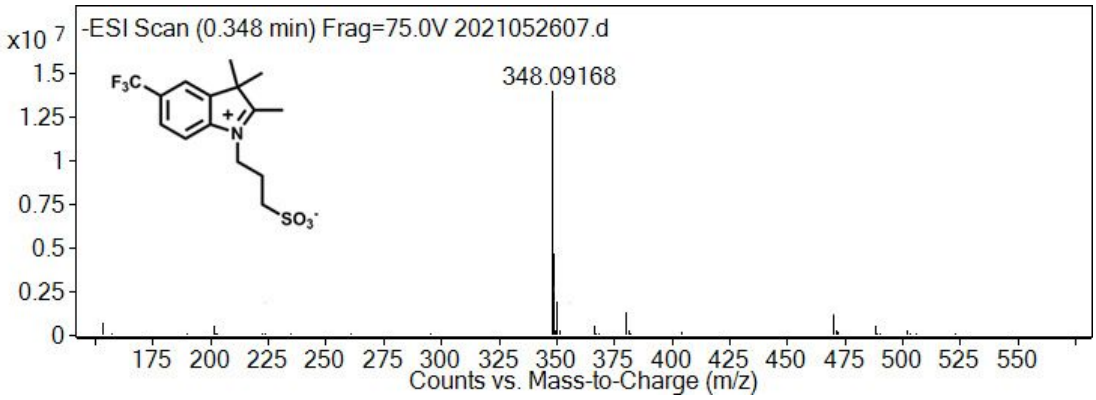

Figure S37. HRMS spectra of compound **3**.

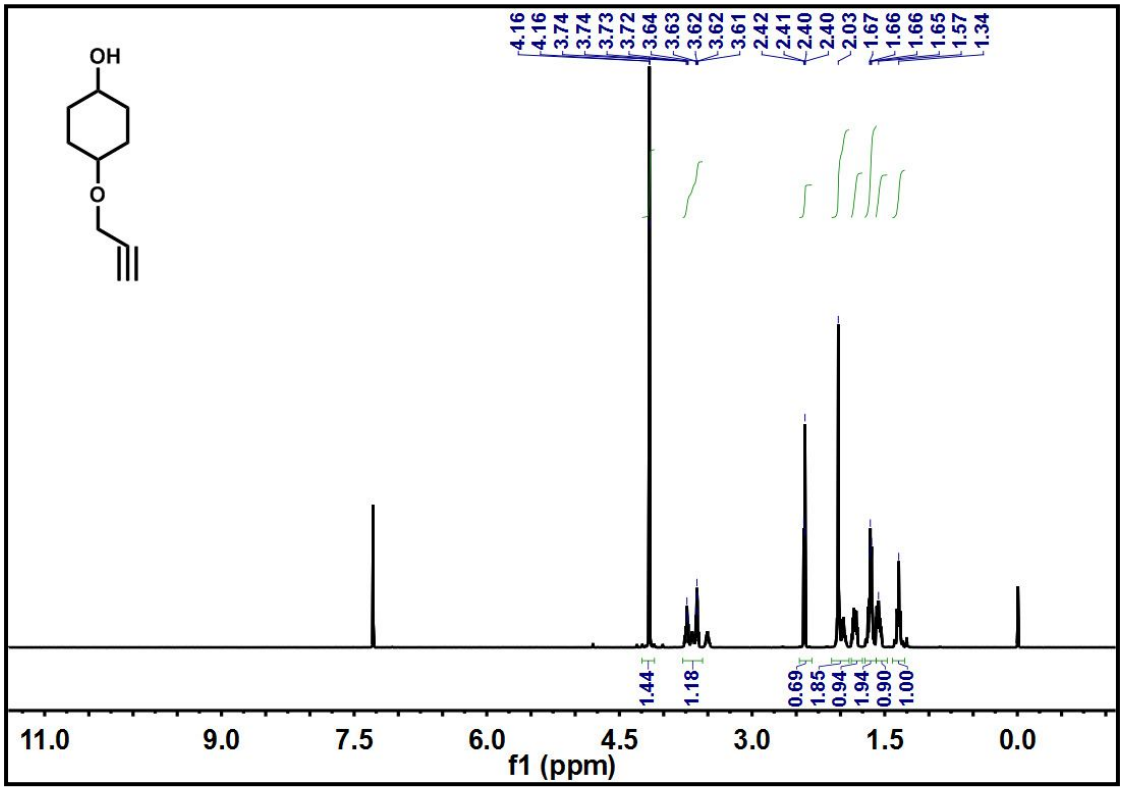

Figure S38. ^{1}H NMR spectra of compound **4** in CD_3OD.

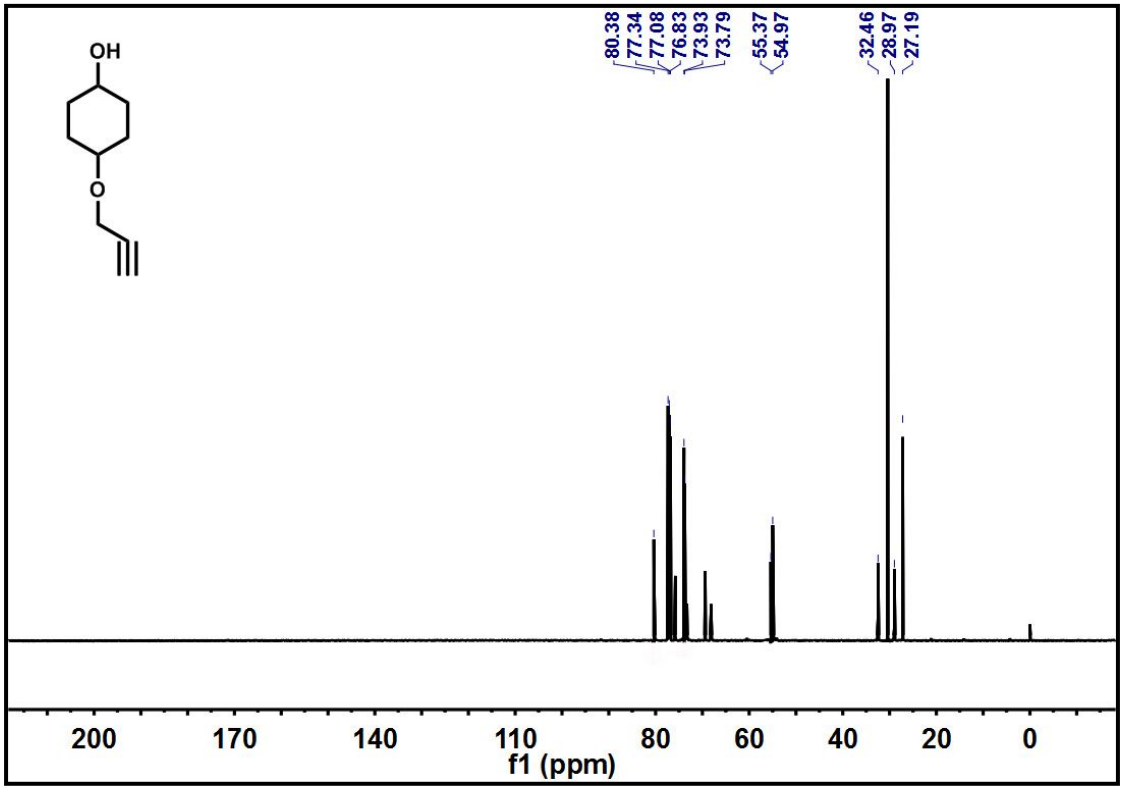

Figure S39. ^{13}C NMR spectra of compound **4** in CD_3OD.

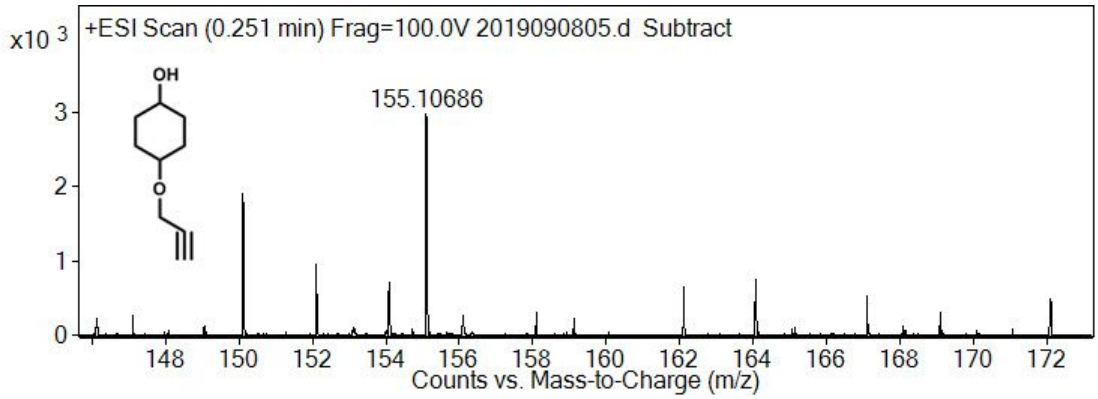

Figure S40. HRMS spectra of compound **4**.

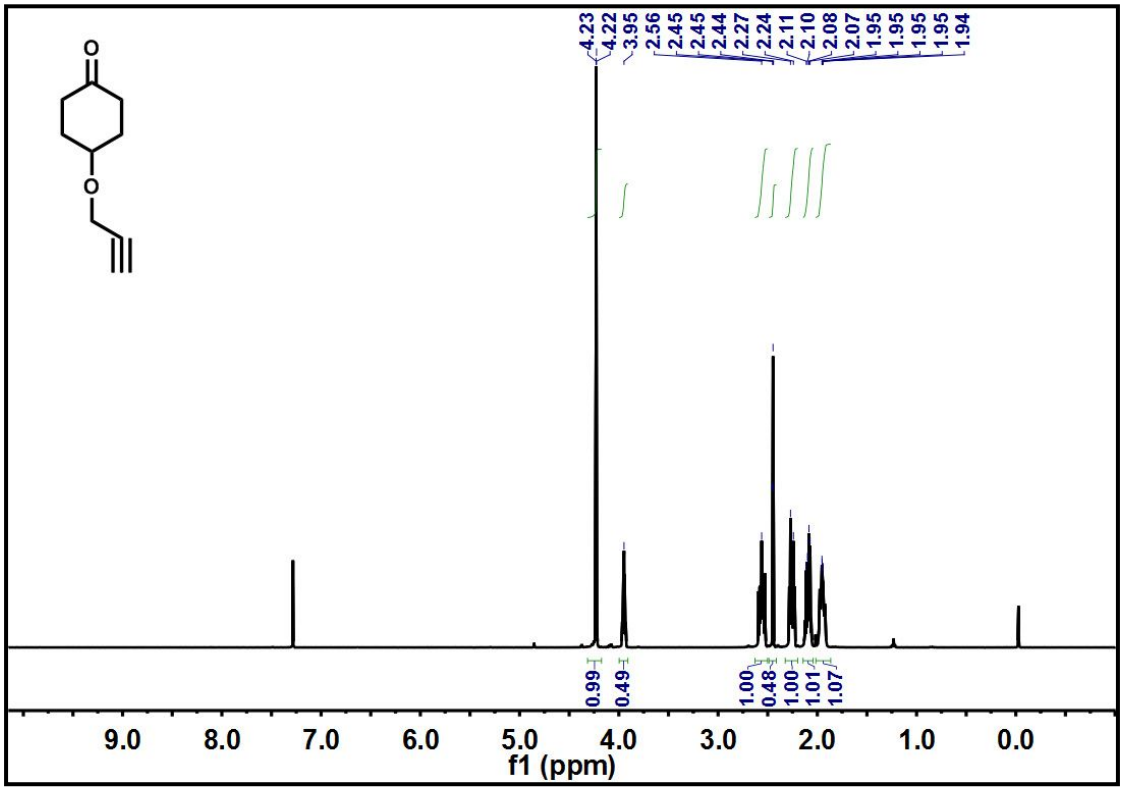

Figure S41. ^{1}H NMR spectra of compound **5** in CD_3OD.

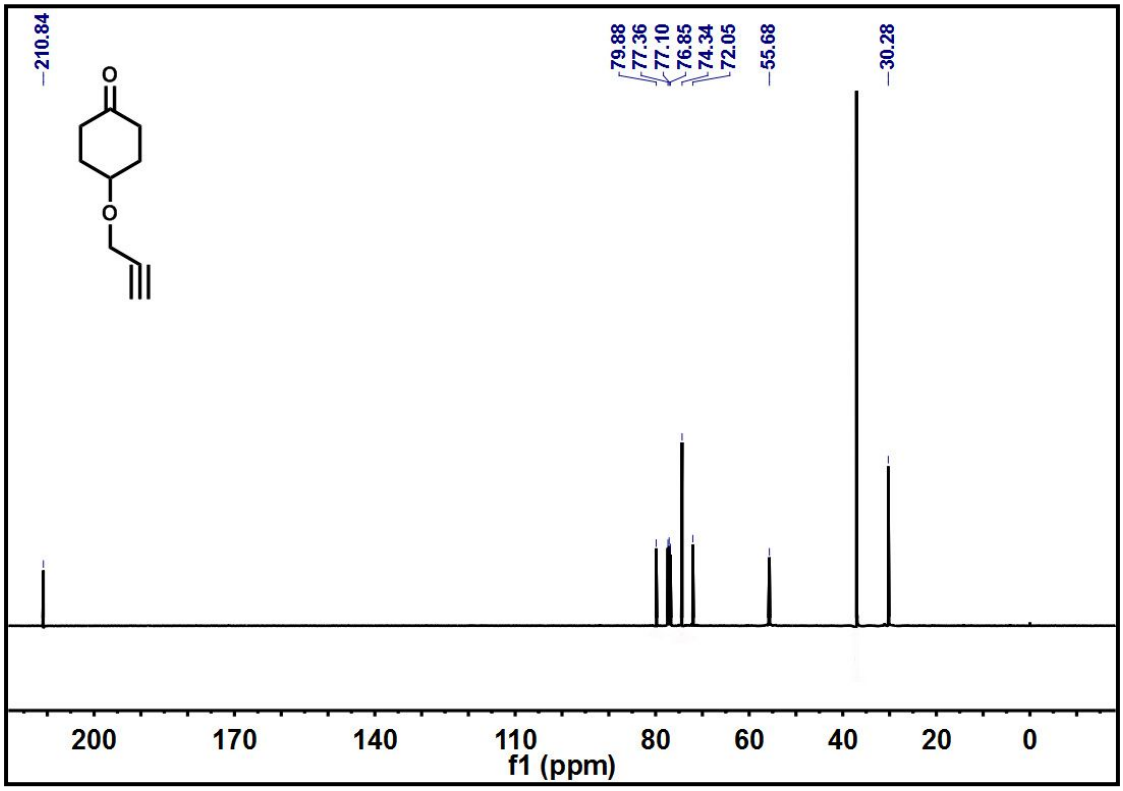

Figure S42. ^{13}C NMR spectra of compound **5** in CD_3OD.

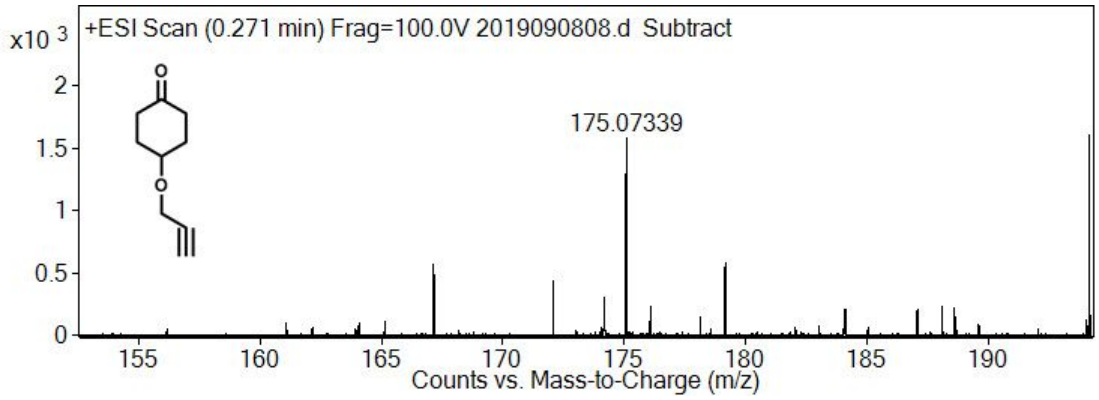

Figure S43. HRMS spectra of compound **5**.

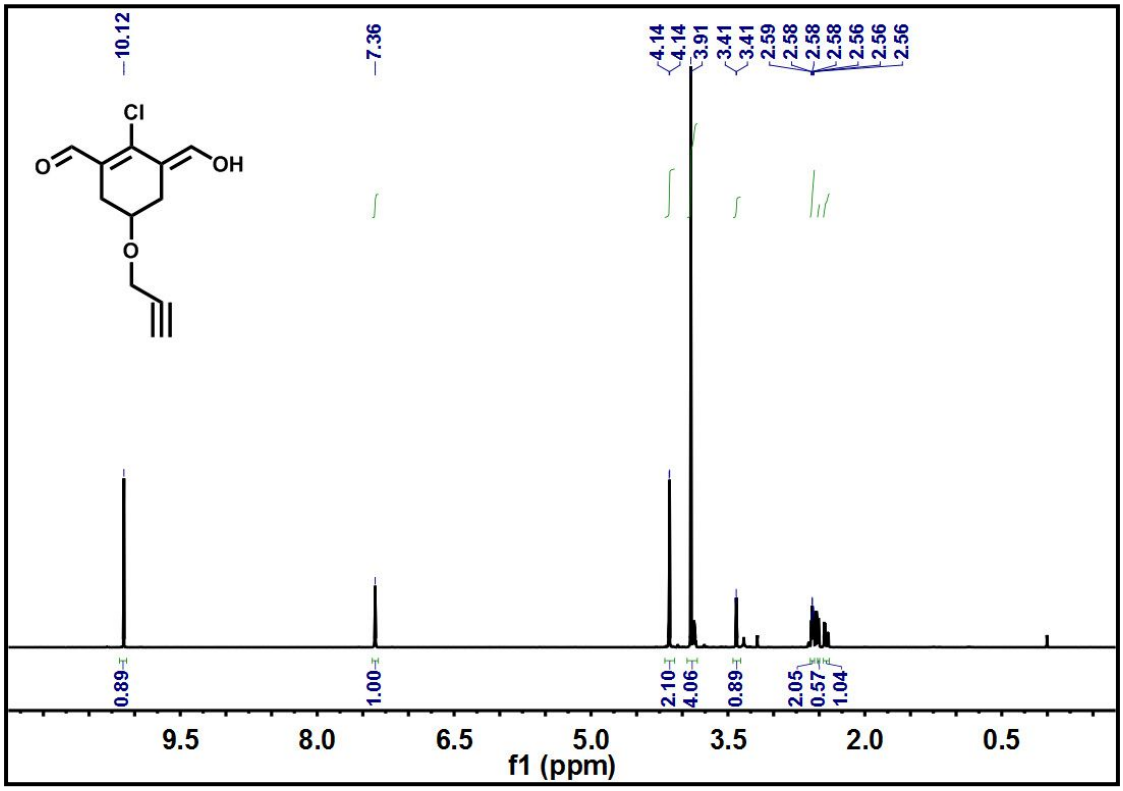

Figure S44. ^{1}H NMR spectra of compound **6** in DMSO-d6.

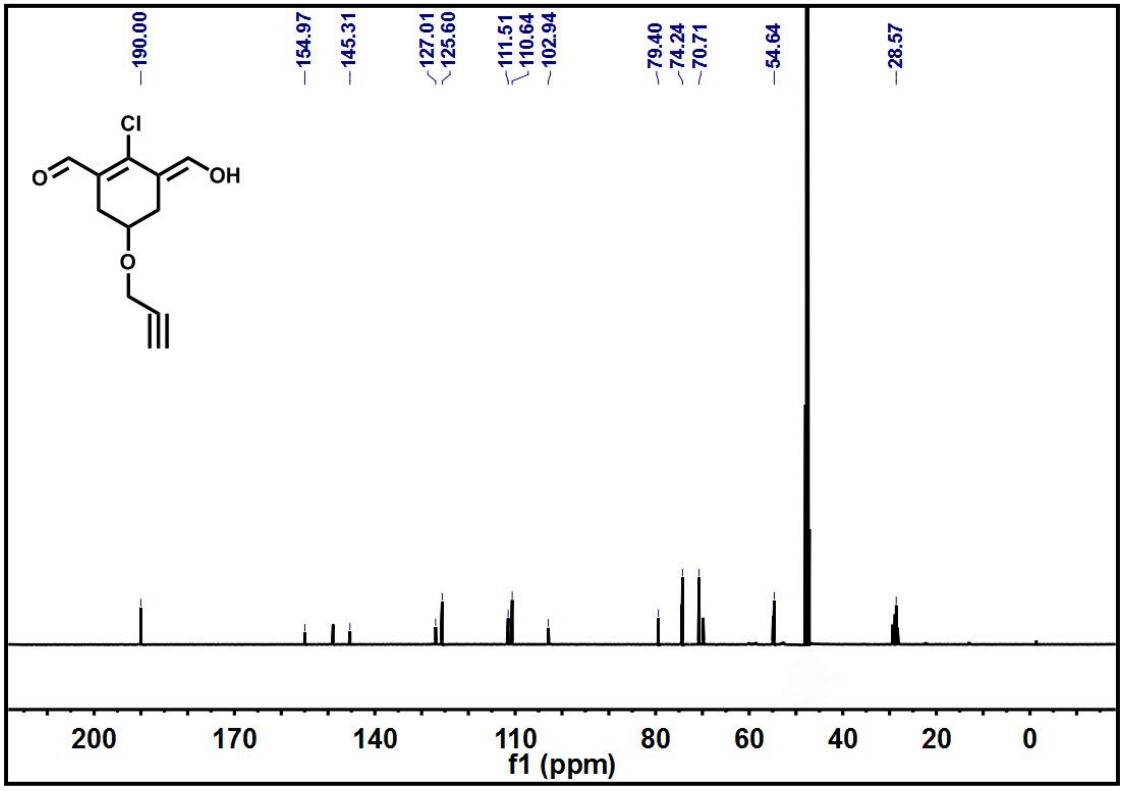

Figure S45. ^{13}C NMR spectra of compound **6** in CD_3OD.

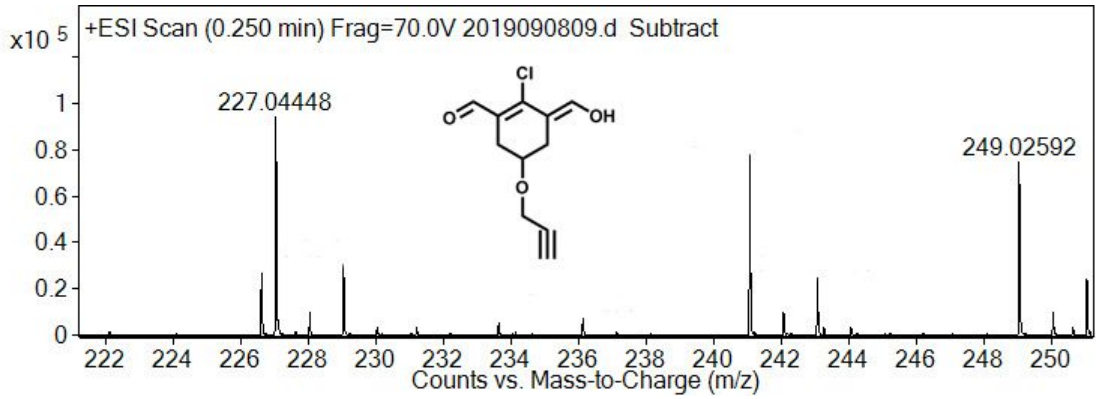

Figure S46. HRMS spectra of compound **6**.

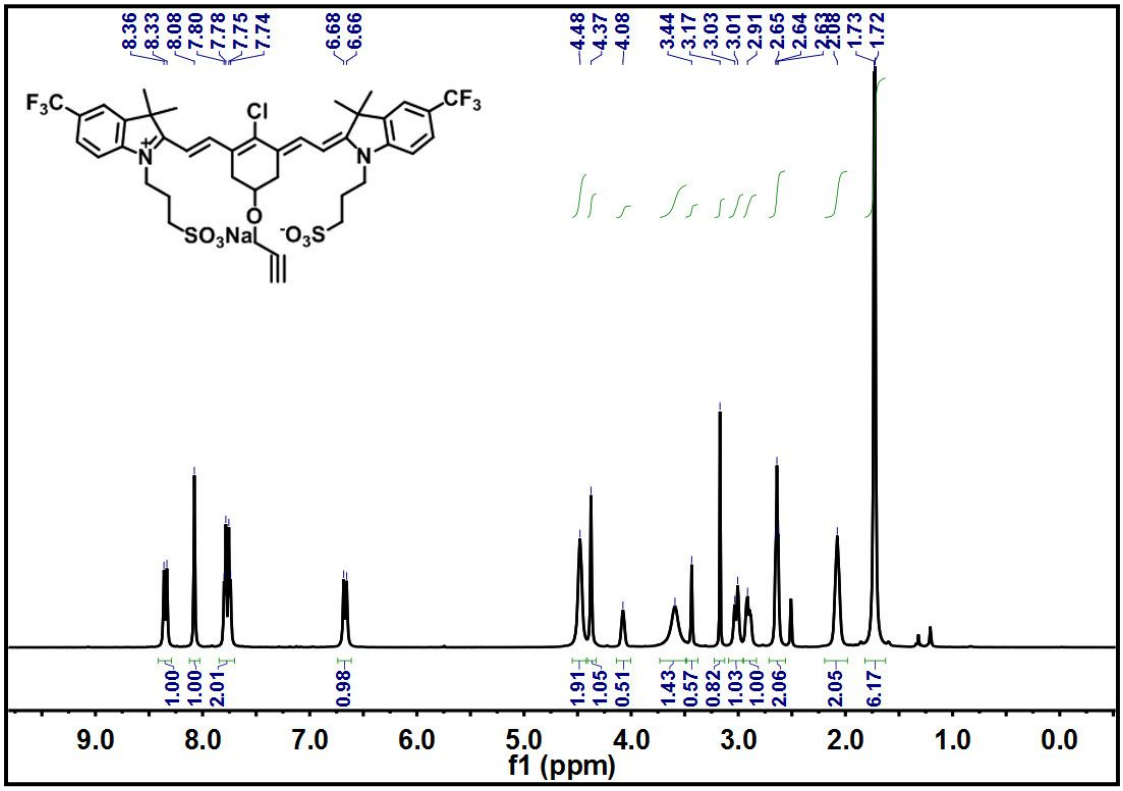

Figure S47. ^{1}H NMR spectra of compound **7** in DMSO-d6.

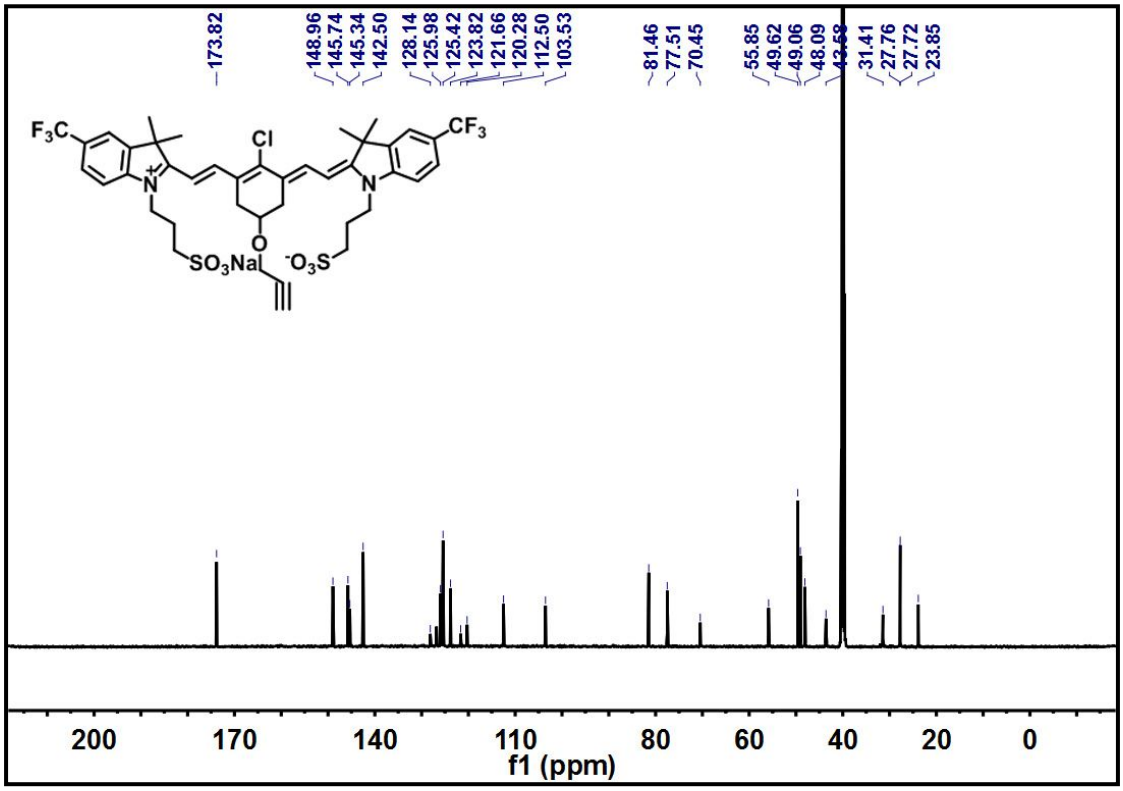

Figure S48. ^{13}C NMR spectra of compound **7** in DMSO-d6.

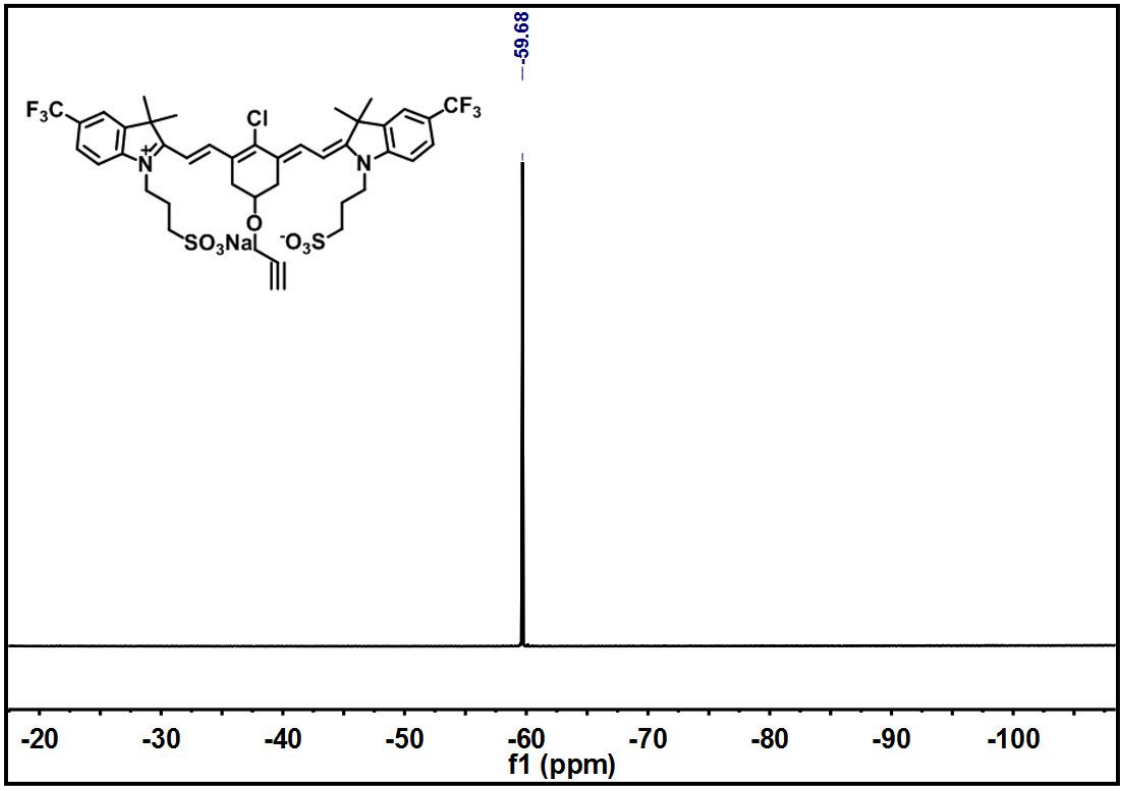

Figure S49. ^{19}F NMR spectra of compound **7** in DMSO-d6.

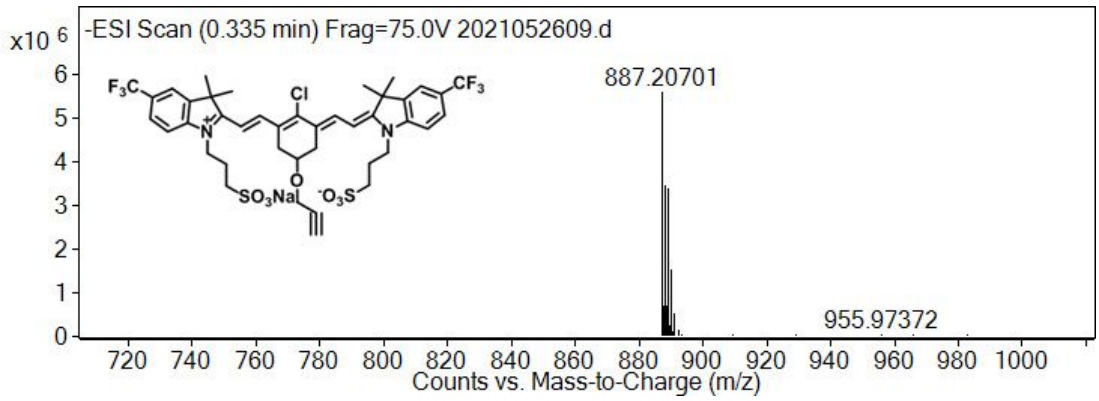

Figure S50. HRMS spectra of compound 7.

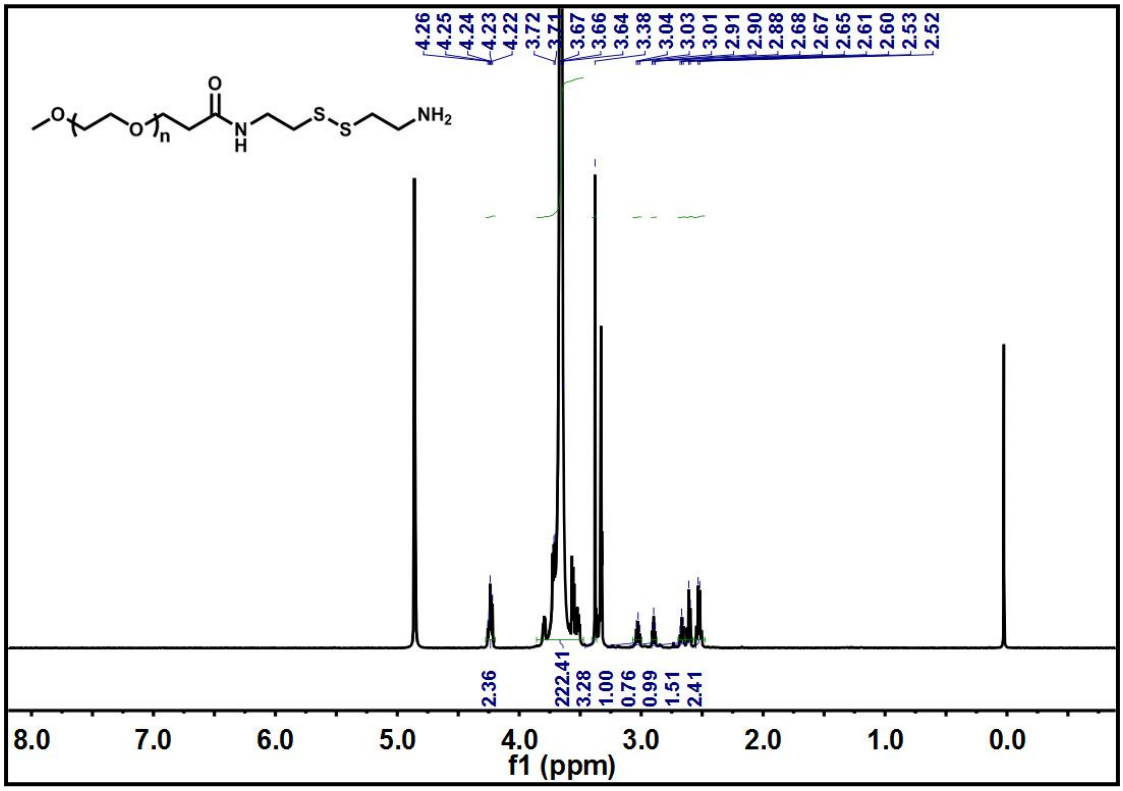

Figure S51. ^{1}H NMR spectra of compound **8** in CD_3OD.

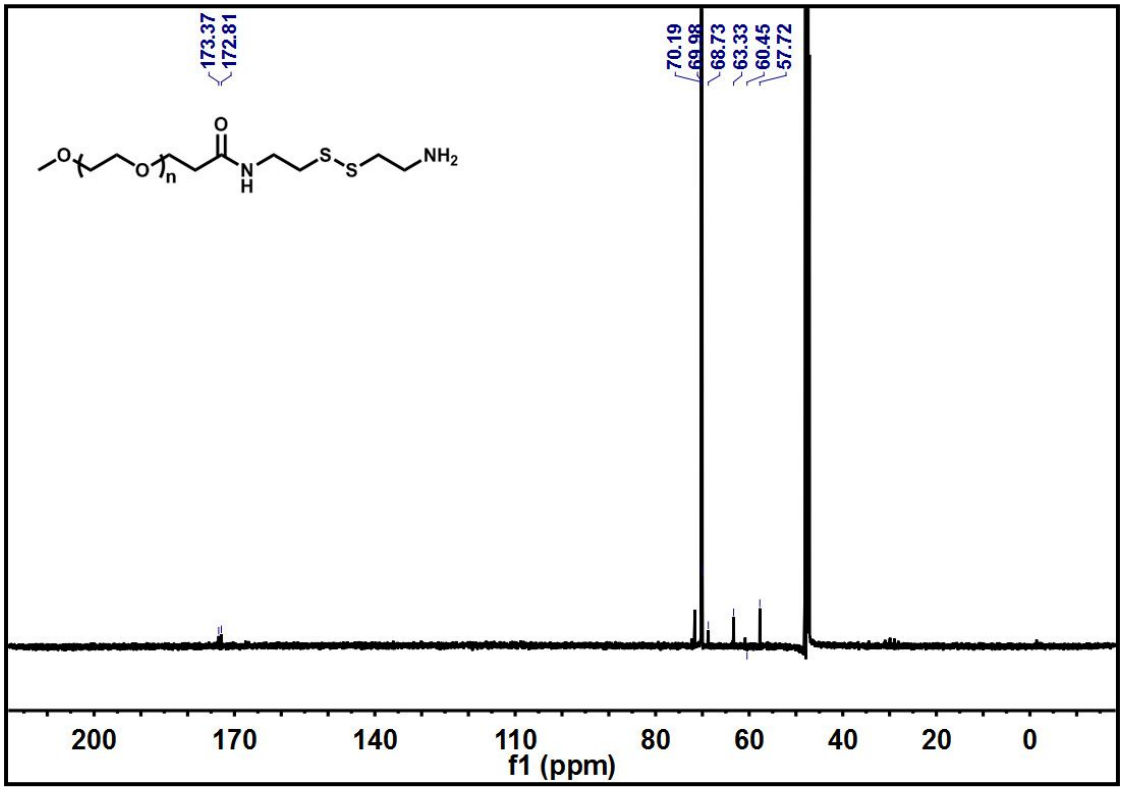

Figure S52. ^{13}C NMR spectra of compound **8** in CD_3OD.

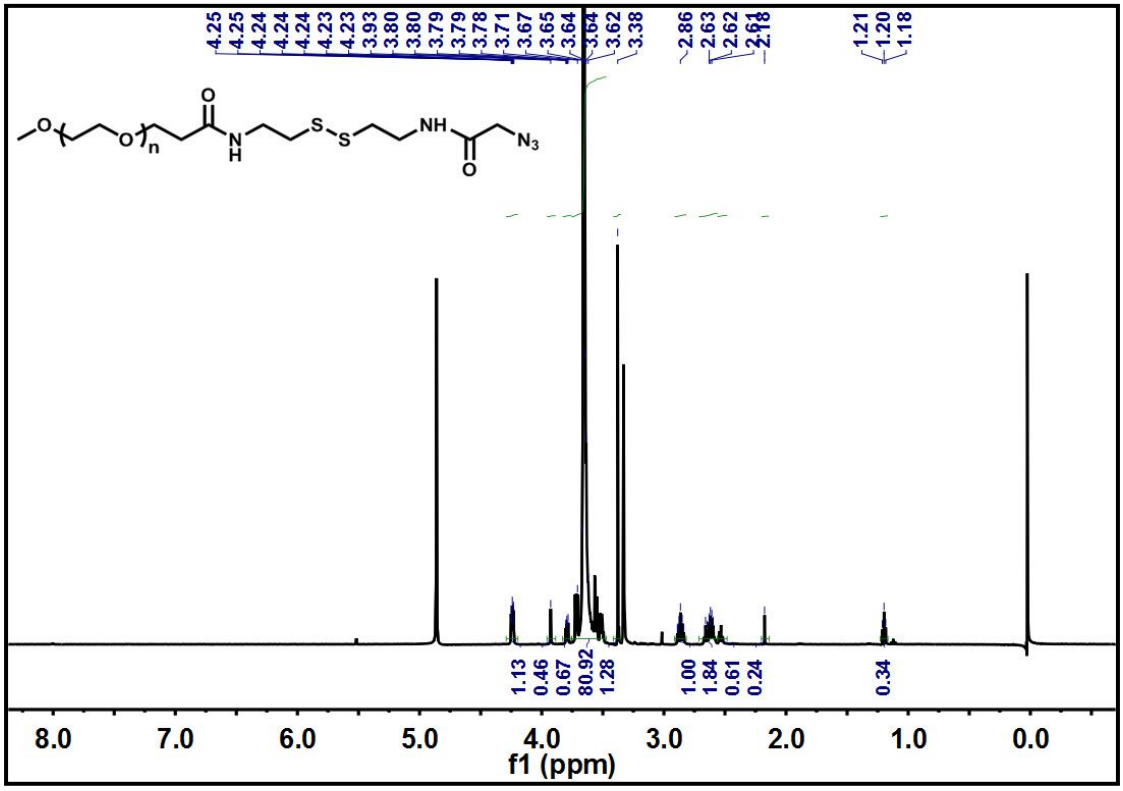

Figure S53. ^{1}H NMR spectra of compound **9** in CD_3OD.

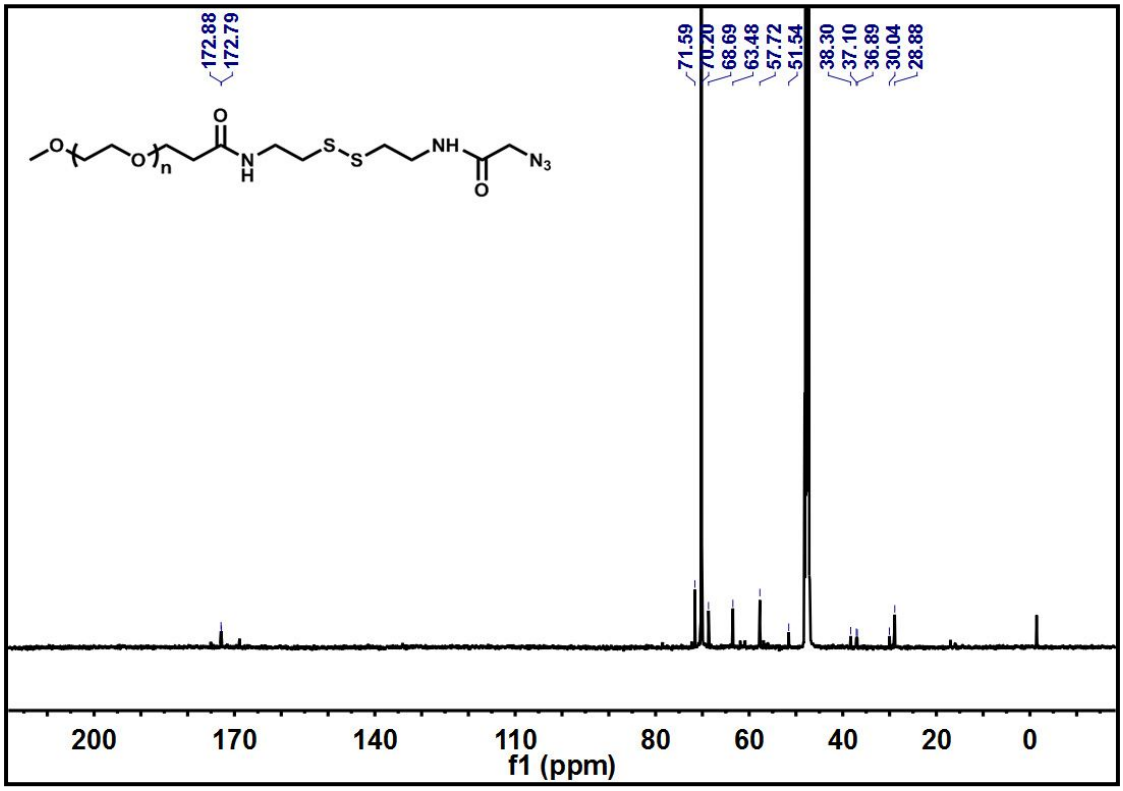

Figure S54. ^{13}C NMR spectra of compound **9** in CD_3OD.

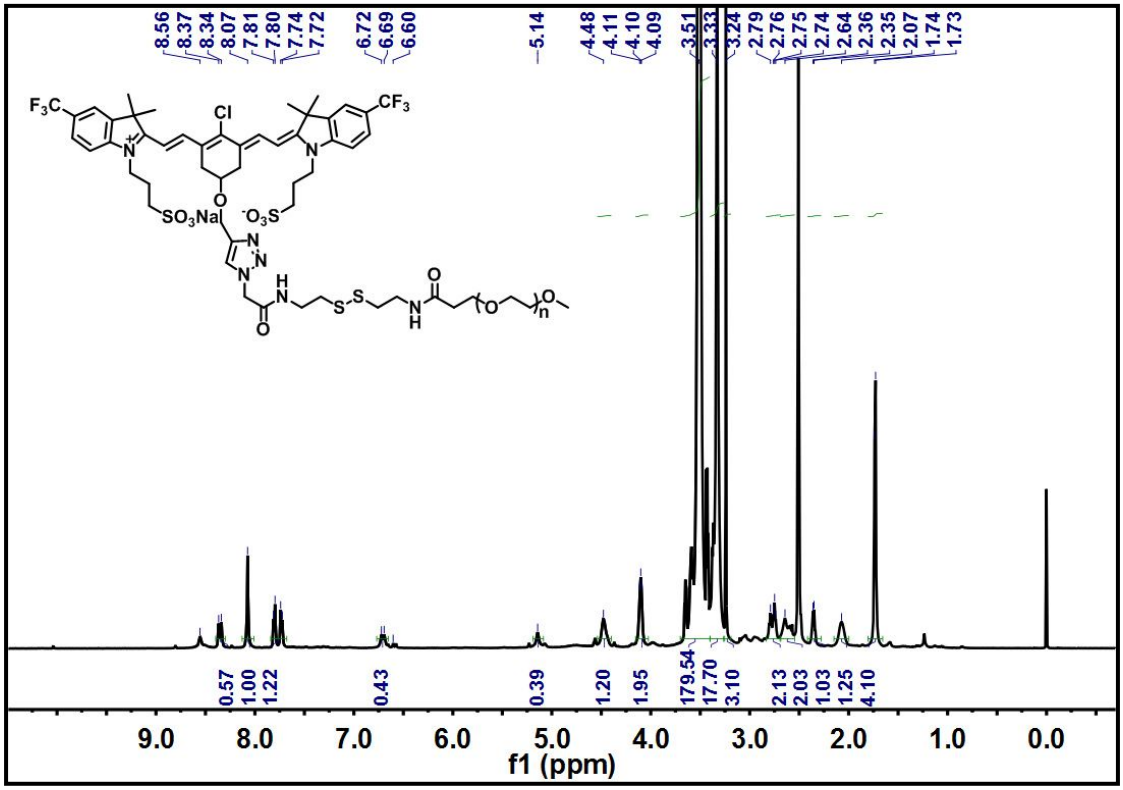

Figure S55. ^{1}H NMR spectra of compound **10** in DMSO-d6.

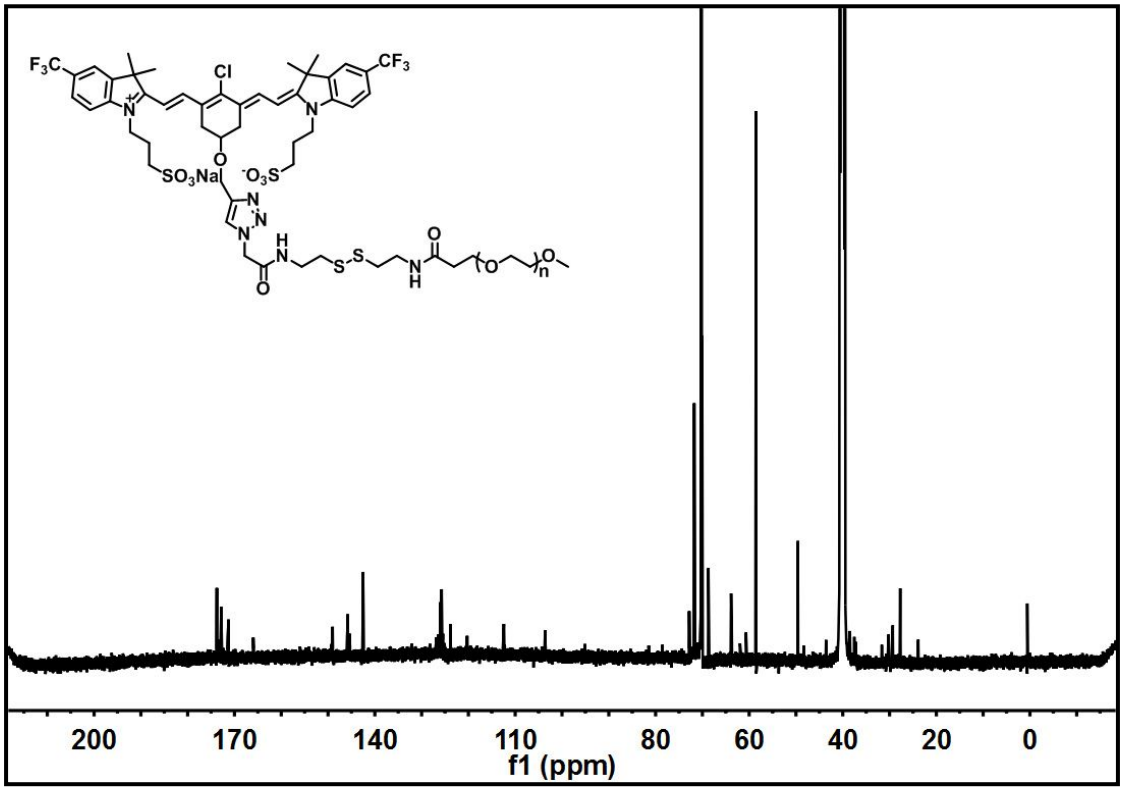

Figure S56. ^{13}C NMR spectra of compound **10** in DMSO-d6.

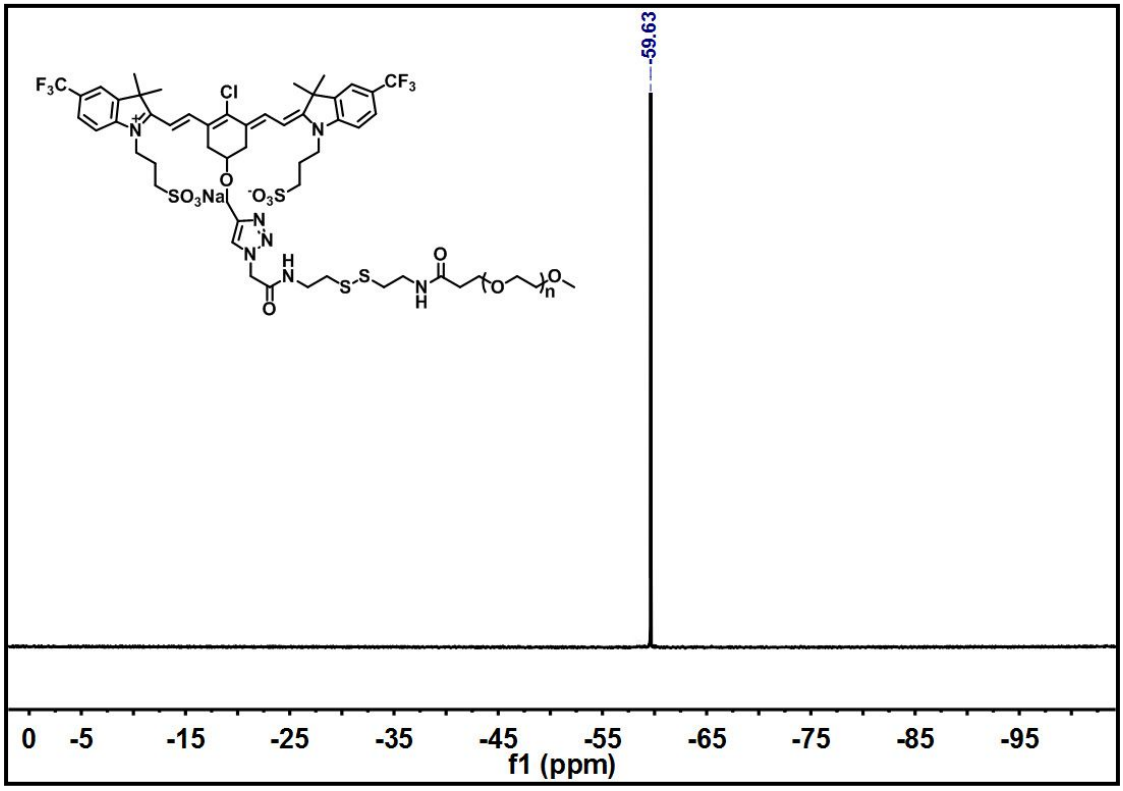

Figure S57. ^{19}F NMR spectra of compound **10** in DMSO-d6.

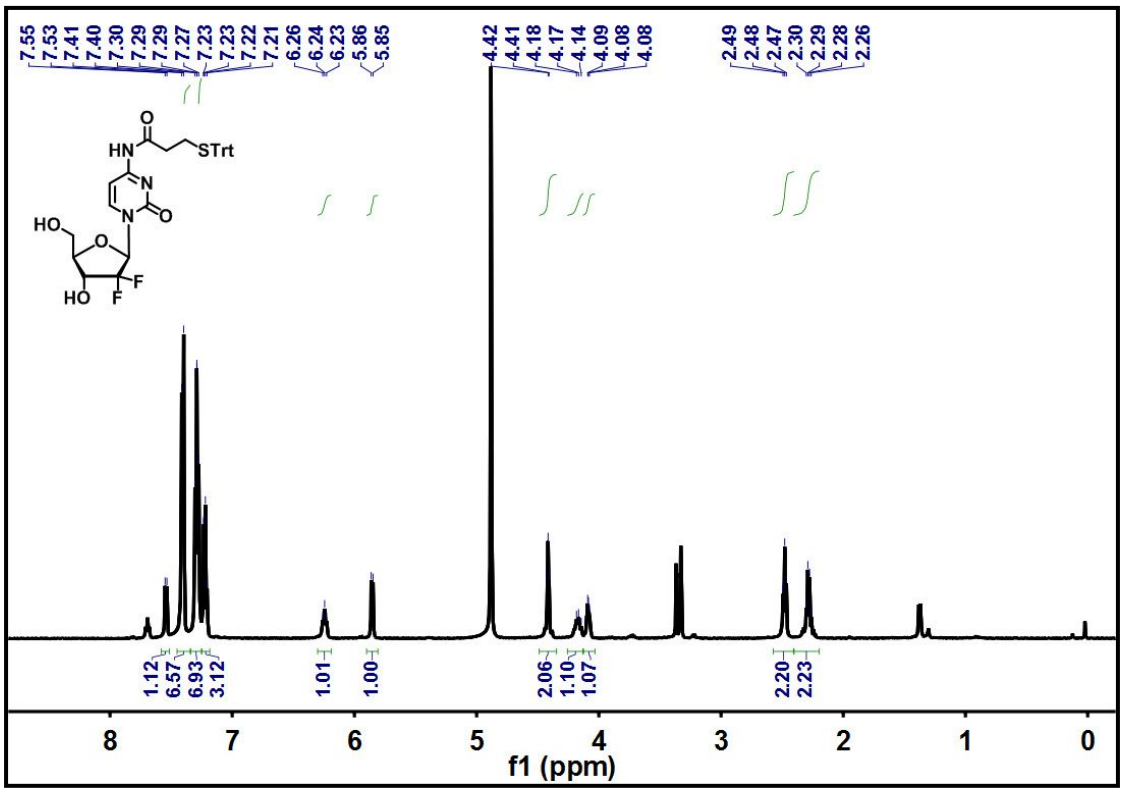

Figure S58. ^{1}H NMR spectra of compound **11** in CD_3OD.

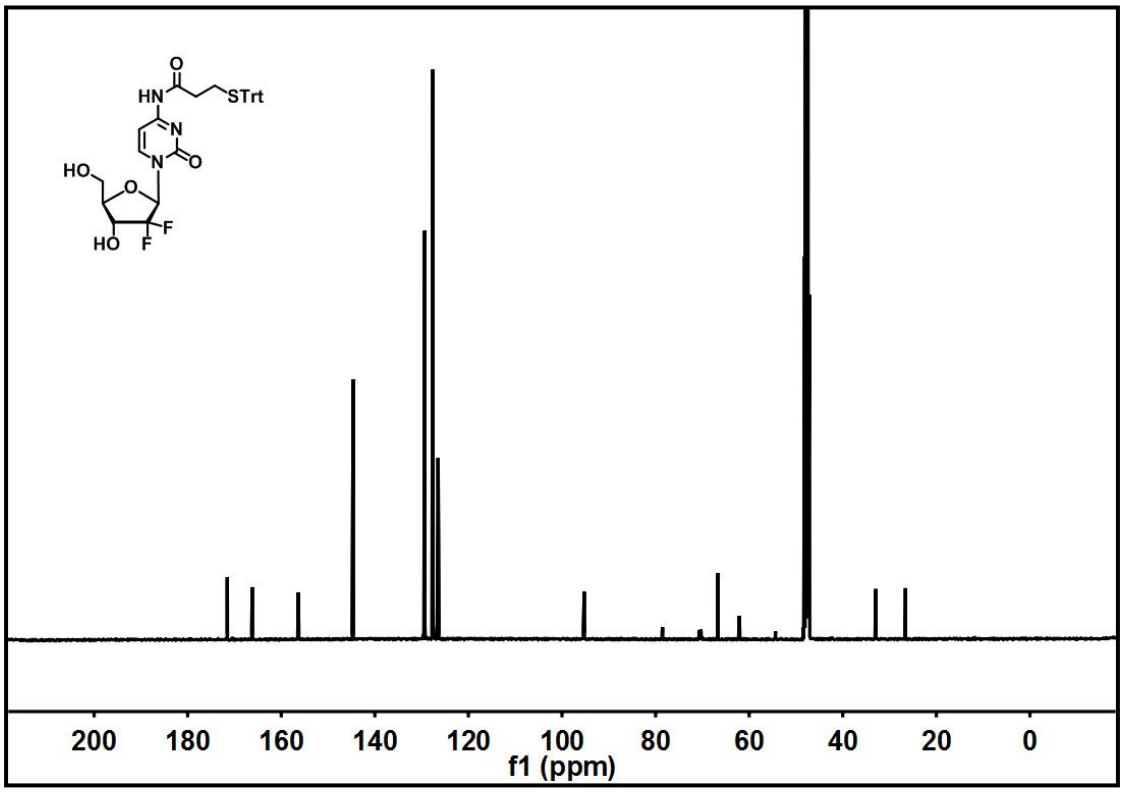

Figure S59. ^{13}C NMR spectra of compound **11** in CD_3OD.

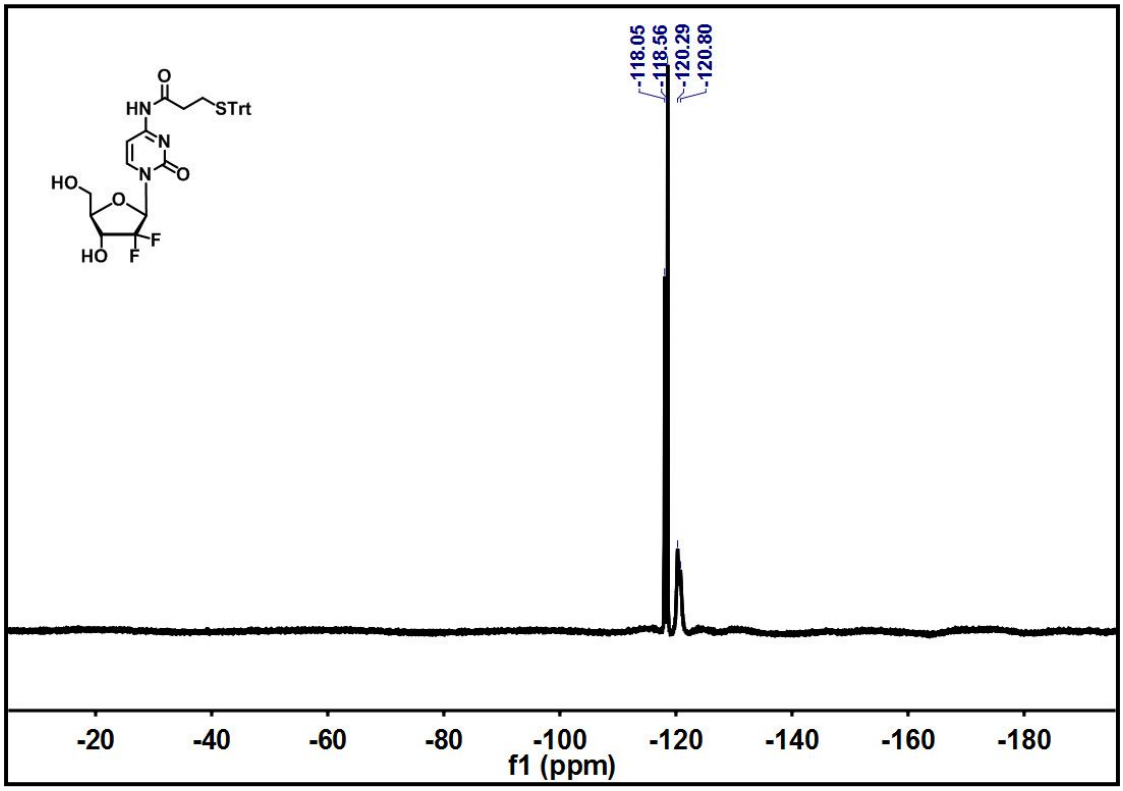

Figure S60. ^{19}F NMR spectra of compound **11** in CD_3OD.

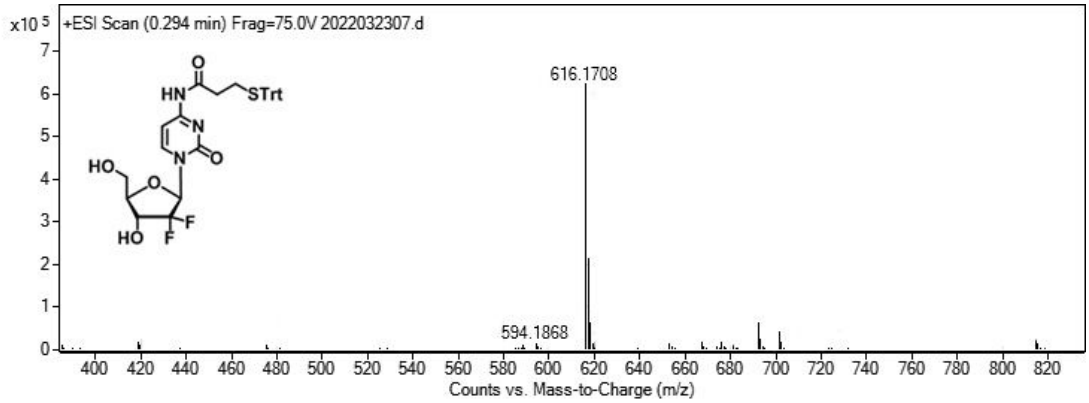

Figure S61. HRMS spectra of compound **11**.

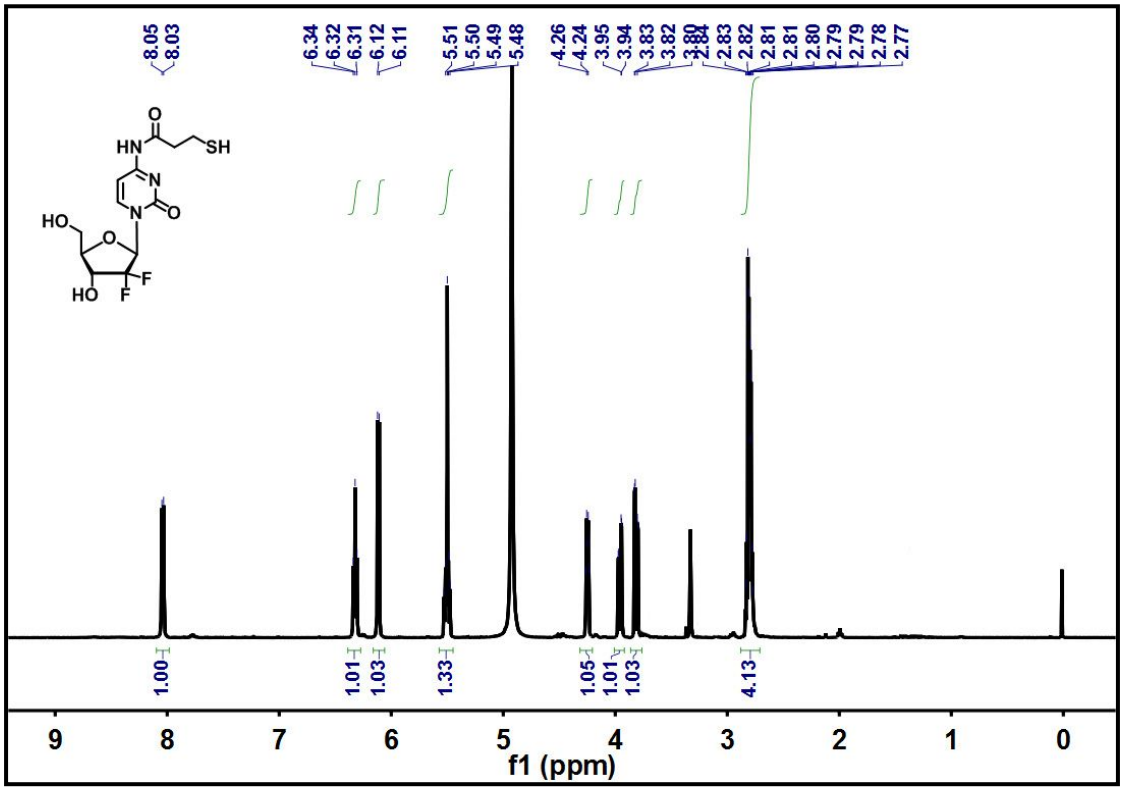

Figure S62. ^{1}H NMR spectra of compound **12** in CD_3OD.

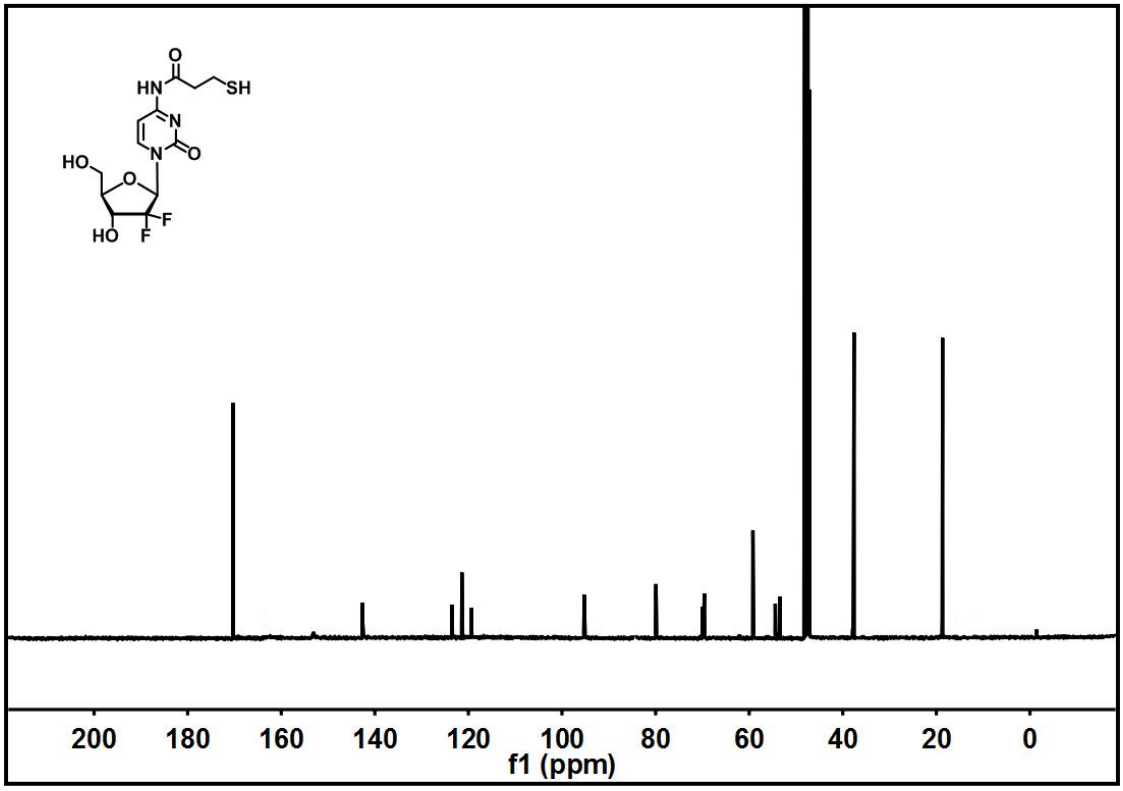

Figure S63. ^{13}C NMR spectra of compound **12** in CD_3OD.

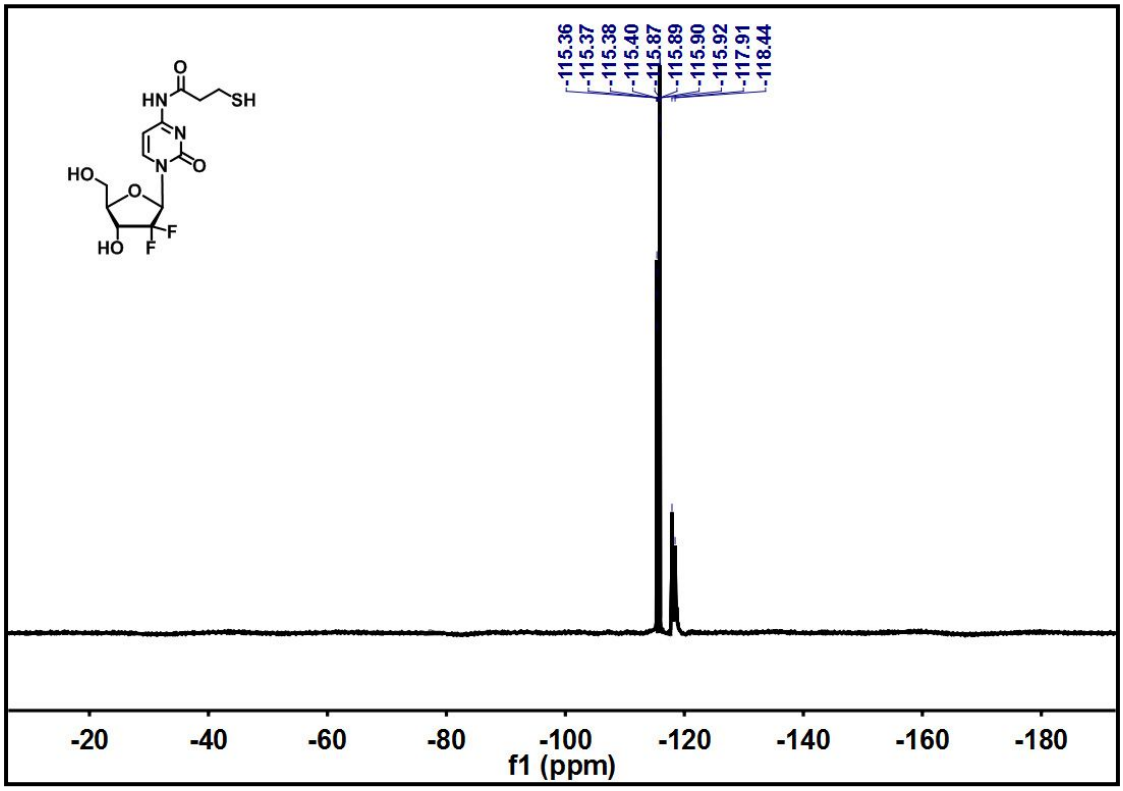

Figure S64. ^{19}F NMR spectra of compound **12** in CD_3OD.

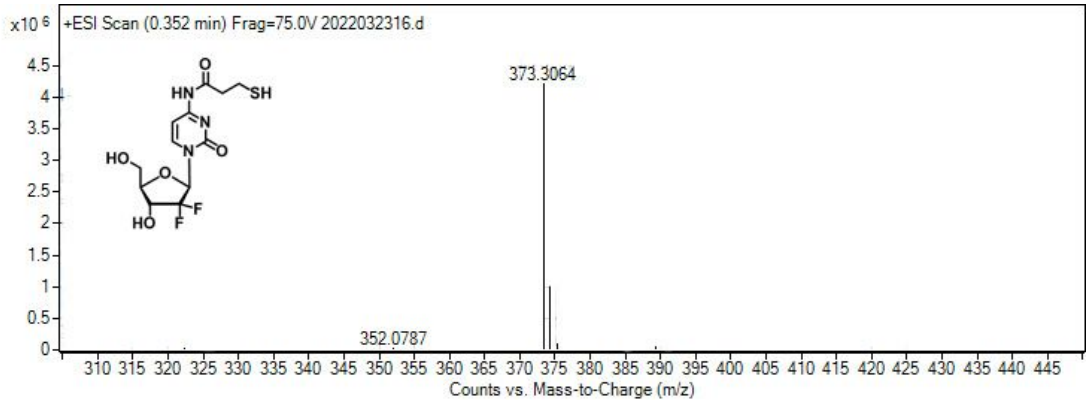

Figure S65. HRMS spectra of compound **12**.

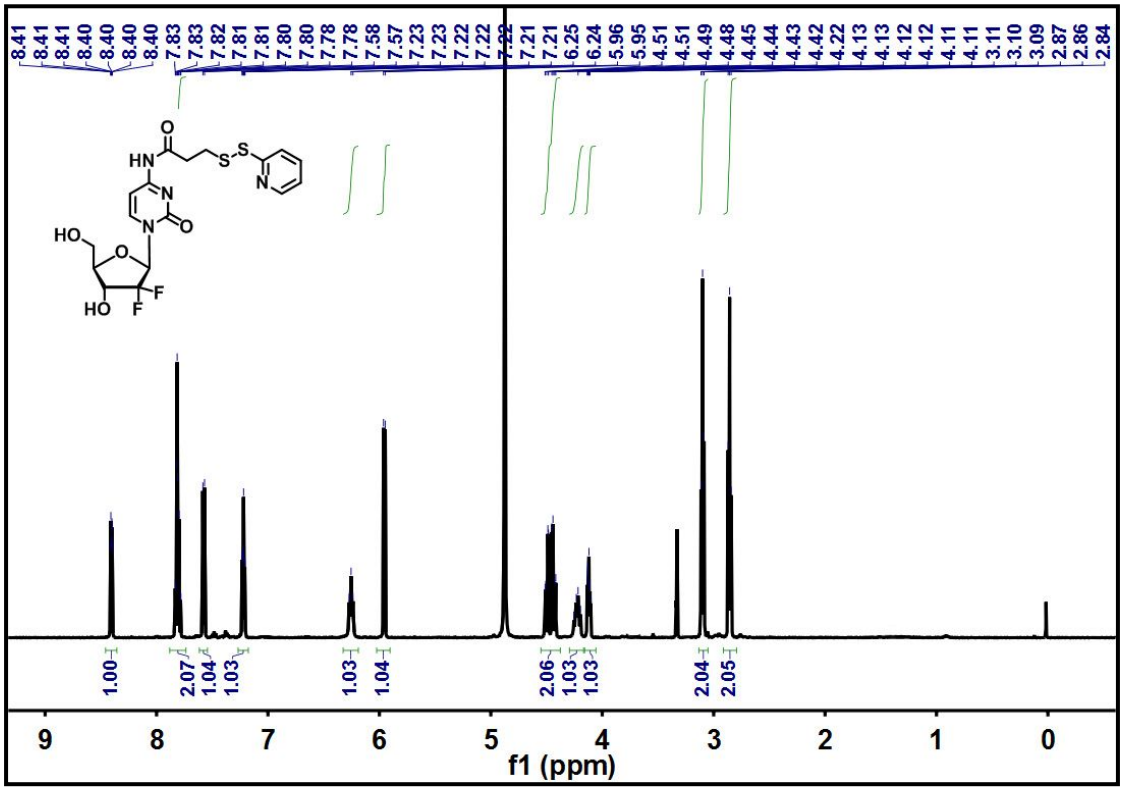

Figure S66. ^{1}H NMR spectra of compound **13** in CD_3OD.

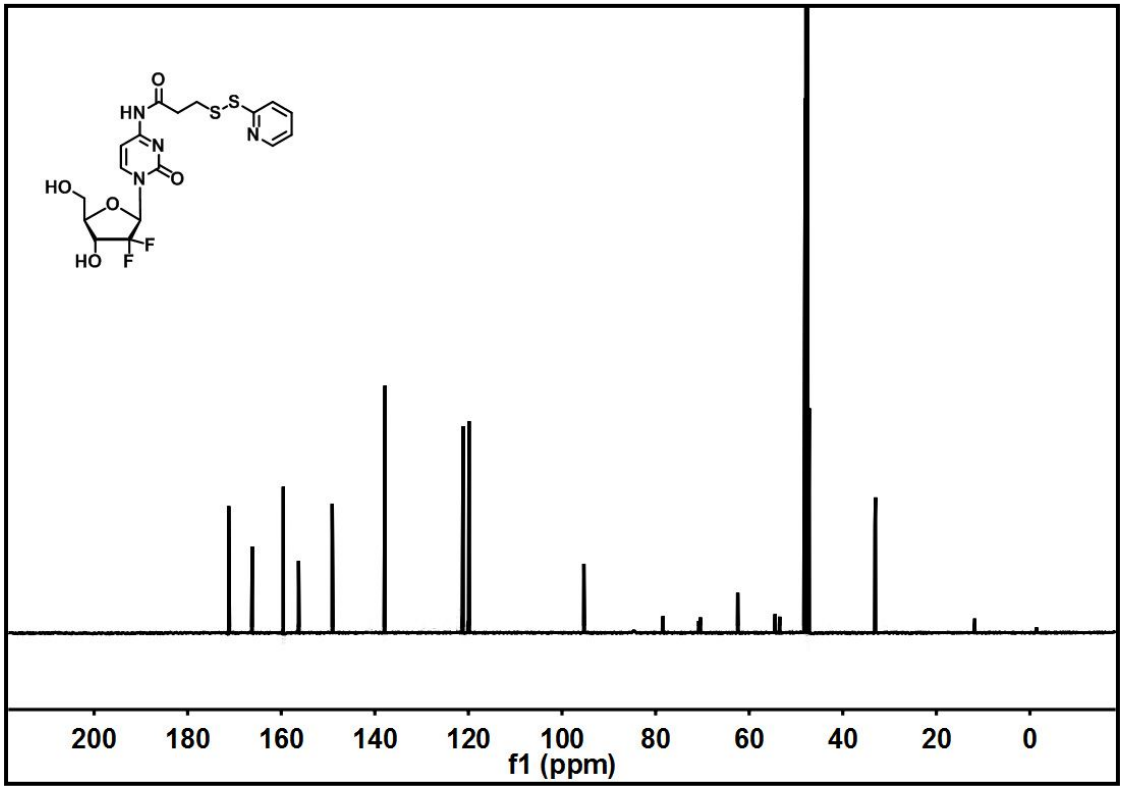

Figure S67. ^{13}C NMR spectra of compound **13** in CD_3OD.

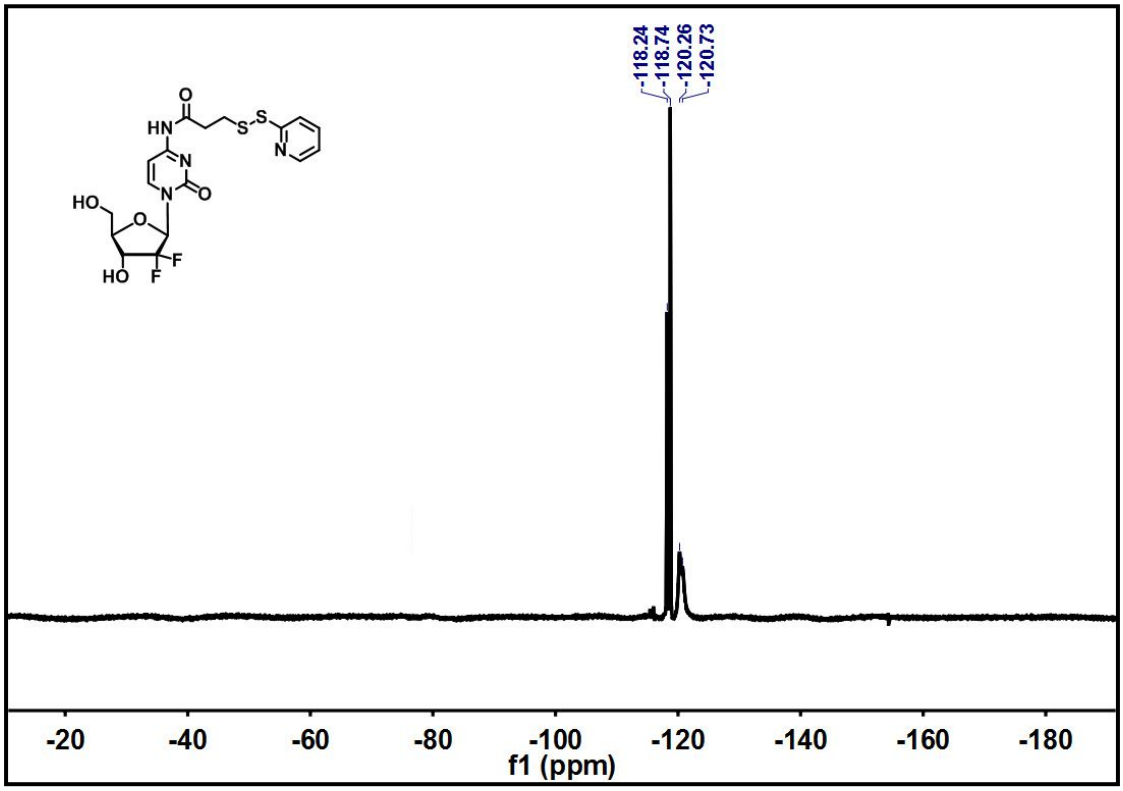

Figure S68. ^{19}F NMR spectra of compound **13** in CD_3OD.

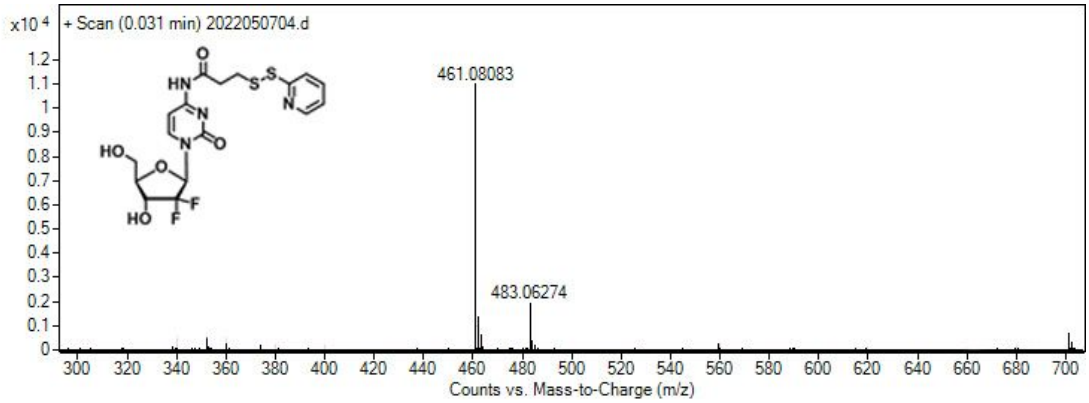

Figure S69. HRMS spectra of compound **13**.

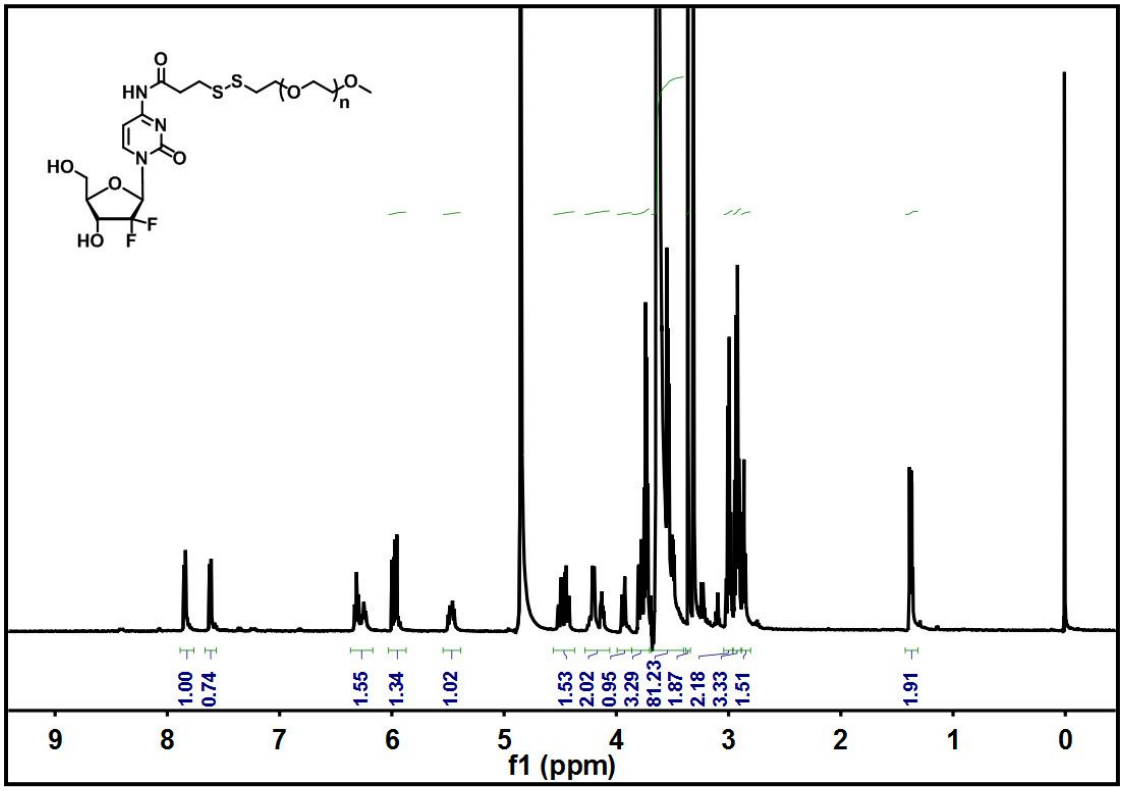

Figure S70. ^{1}H NMR spectra of compound **14** in CD_3OD.

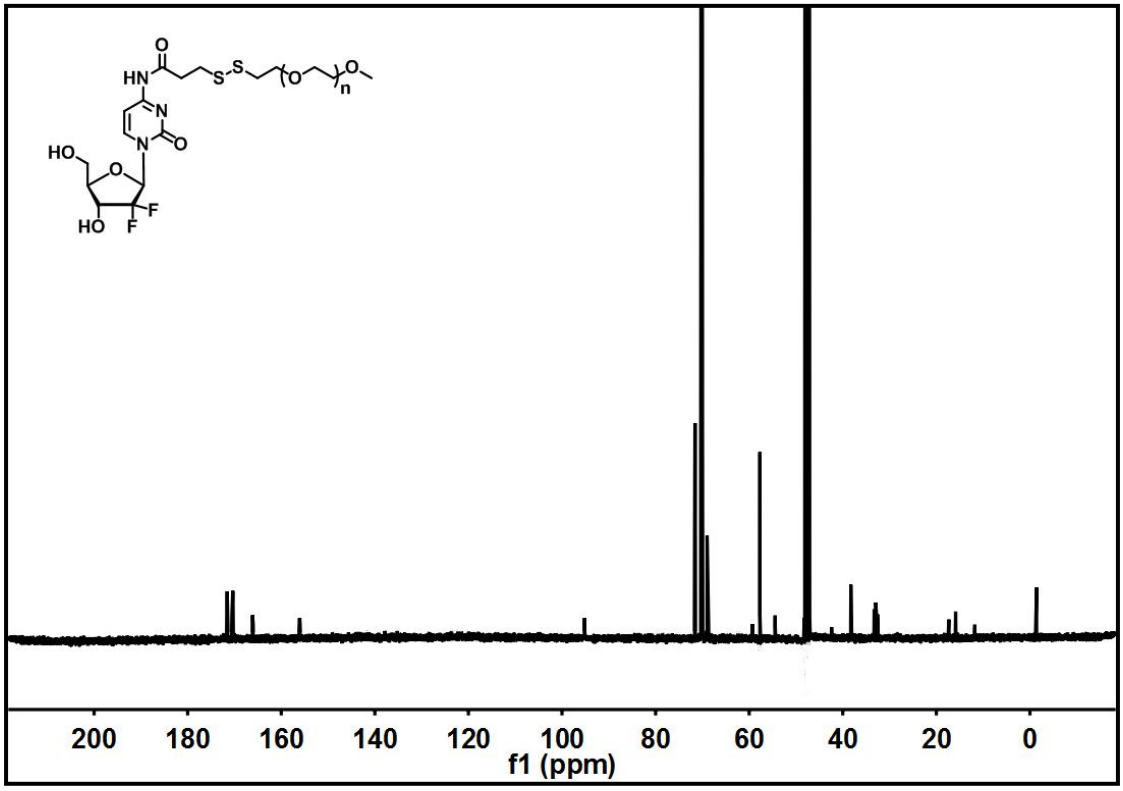

Figure S71. ^{13}C NMR spectra of compound **14** in CD_3OD.

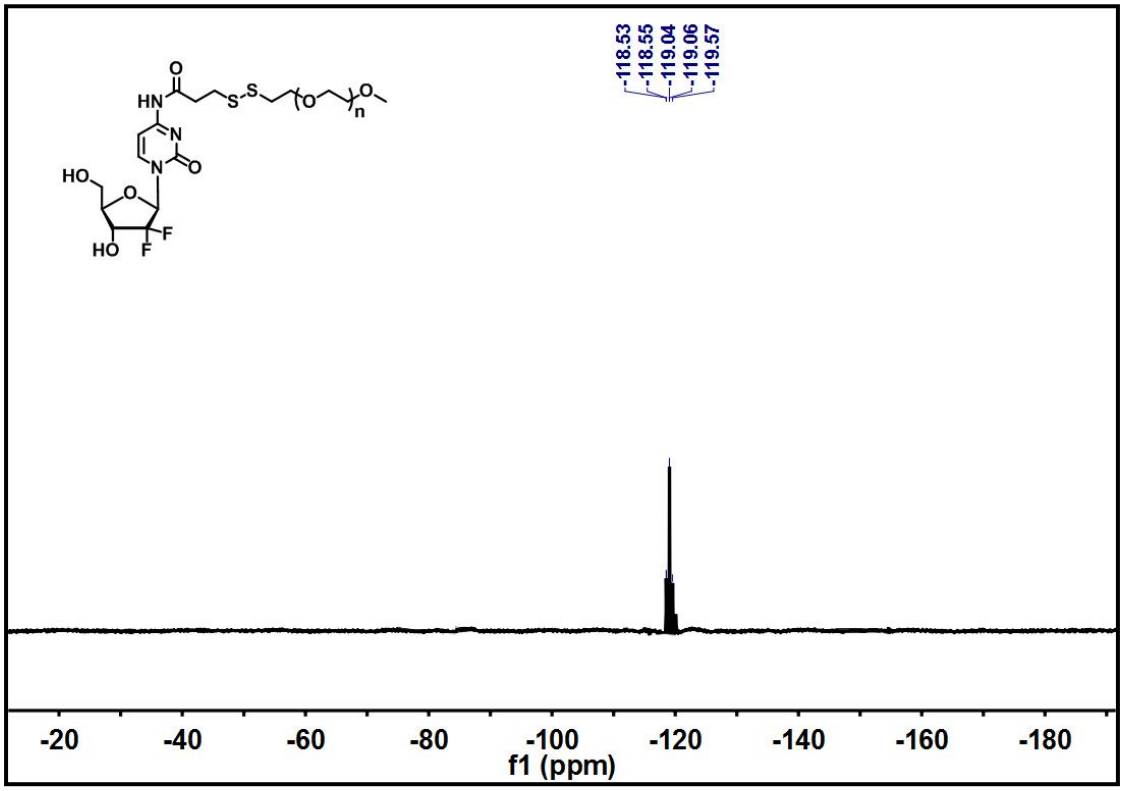

Figure S72. ^{19}F NMR spectra of compound **14** in CD_3OD.